Euro. Jnl of Applied Mathematics (2012), *vol.* 23, *pp.* 3–28.
doi:10.1017/S0956792510000355

A criterion for symmetric tricritical points in condensed ordered phases

F. BISI[1,2], E. C. GARTLAND, JR.[3] and E. G. VIRGA[1]

[1]*Dipartimento di Matematica, Università di Pavia, Via Ferrata 1, 27100 Pavia, Italy*
email: eg.virga@unipv.it

[2]*Laboratory of Applied Mathematics, Fondazione Università di Mantova, Via Scarsellini 2, 46100 Mantova, Italy*
email: fulvio.bisi@unipv.it

[3]*Department of Mathematical Sciences, Kent State University, Kent, OH 44242, USA*
email: gartland@math.kent.edu

(*Received 24 November 2010; revised 30 November 2010; accepted 1 December 2010; first published online 5 January 2011*)

Basic methods from bifurcation theory are applied to derive a criterion that predicts when a symmetric tricritical point may occur in a transition between condensed ordered phases described by any finite number of scalar order parameters. At such a point, a change of order takes place in the phase transition, which passes from first to second order, or *vice versa*.

Key words: Phase transitions; Critical points of functions and mappings; Bifurcation problems; Bifurcations and instability; Computational methods for bifurcation problems

1 Introduction

The study of equilibrium phases in ordered systems and their transitions is intimately related to the theory of critical points and their bifurcations. The mathematical theory of bifurcation can shed light on the physical understanding of phase transitions, as the connection between these two realms is far more than semantic. Here we apply the methods of bifurcation theory to a peculiar aspect of critical phenomena, namely, to the change of order in a phase transition upon varying control or model parameters.

We are interested in aspects of phase transitions in bulk samples of ordered materials, such as liquid crystals. In a mathematical model of such a system, the phase is typically represented by a finite number of scalar variables, or 'order parameters', and the transition from one phase to another occurs when one or more material or control parameters pass through certain critical values. The information is usually organised in a 'phase diagram'. See for example [18, 30, 31]. A particular example that we have in mind (which is described in a later section) concerns the phases of a biaxial liquid crystal, which can be 'isotropic' (disordered) at high temperatures and either 'uniaxial nematic' or 'biaxial nematic' (orientationally ordered) at lower temperatures, depending on the values of certain material biaxiality parameters.

In the areas of liquid crystals and other related condensed-matter systems, the term 'tricritical point' has come to signify a point in a phase diagram at which the nature of a phase transition changes from 'first order' (associated with a discontinuous change in at least one of the order parameters) to 'second order' (in which all order parameters

change continuously). This terminology appears to derive from the usage in physical chemistry concerned with multi-component fluid mixtures. There the term 'tricritical point' specifically refers to a scenario in which the change in the phase transition comes about when three coexisting fluid phases coalesce into one. This generalises the term 'critical point', in which two coexisting phases coalesce. If more than three coexisting phases coalesce, the point is referred to as a 'multicritical point'. The point is said to be a 'symmetric' tricritical (or multicritical) point if all but one of the phases are related to each other through some symmetry of the system. See for example [4, 10–12, 16, 17].

The connection between coalescing phases and the first-order *vis-à-vis* second-order nature of associated phase transitions can be illustrated by simple Landau expansions. Consider the two different model free energies

$$F_1(\psi) = \beta\psi^2 + a_3\psi^3 + \psi^4\,, \quad F_2(\psi) = \beta\psi^2 + a_4\psi^4 + \psi^6.$$

Here one should think of ψ as an order parameter, the non-zero values of which indicate some degree of order in the system, β as a control parameter (such as temperature) and a_3 and a_4 as material parameters (which can differ from one type of material or mixture to another). Equilibrium states are solutions of $F'(\psi) = 0$:

$$\begin{aligned} F_1'(\psi) = 0 \quad &\Leftrightarrow \quad \psi = 0 \ \text{ or } \ 2\beta + 3a_3\psi + 4\psi^2 = 0\,, \\ F_2'(\psi) = 0 \quad &\Leftrightarrow \quad \psi = 0 \ \text{ or } \ \beta + 2a_4\psi^2 + 3\psi^4 = 0\,. \end{aligned}$$

Equilibria are *stable* if they provide the global free-energy minimum, $F(\psi^*) = \min_\psi F(\psi)$; they are *metastable* (or locally stable) if they give a local minimum.

For the free energy F_1, with $a_3 < 0$, the system undergoes a first-order phase transition at a value $\beta = \beta^* > 0$, with the coexisting phases $\psi = 0$ and $\psi = \psi^* > 0$. As $a_3 \to 0$, these two phases coalesce, and the phase transition becomes second order at $\beta^* = 0$. See Figure 1 (left). For F_2, with $a_4 < 0$, the system again undergoes a first-order phase transition at some $\beta^* > 0$, this time with three coexisting phases: $\psi = 0$ and $\psi = \pm\psi^*$, $\psi^* > 0$. As $a_4 \to 0$, these three phases coalesce, and the phase transition again becomes second order at $\beta^* = 0$. See Figure 1 (right). In the terminology of Griffiths and Widom [10–12], the former case corresponds to a 'critical point', while the latter case is a 'symmetric tricritical point'.

In this paper, we are concerned with indicator functions that can be used to identify points in a bifurcation diagram where a potential change from a first-order to a second-order phase transition could occur in the presence of a reflectional symmetry breaking. This is a common and important scenario in such ordered materials. In keeping with the terminology discussed above, we define a *symmetric tricritical point* to be a point at which a first-order phase transition becomes second-order in the presence of a reflectional symmetry breaking.

This is made more precise in Section 2, where we first recall basic facts from bifurcation theory, phrased in the language adopted in the rest of the paper. In Section 3, we derive a tricriticality criterion from the general bifurcation equations that applies to a bifurcation breaking the reflectional symmetry enjoyed by the free energy, F. Though our analysis is performed under rather general hypotheses, it becomes much neater when the Hessian $\mathbf{H}_0$ of F at a symmetry-breaking bifurcation point has a one-dimensional null space $\mathbb{K}$, a case that shall be treated throughout in greater detail. This case applies in particular to

https://doi.org/10.1017/S0956792510000355 Published online by Cambridge University Press

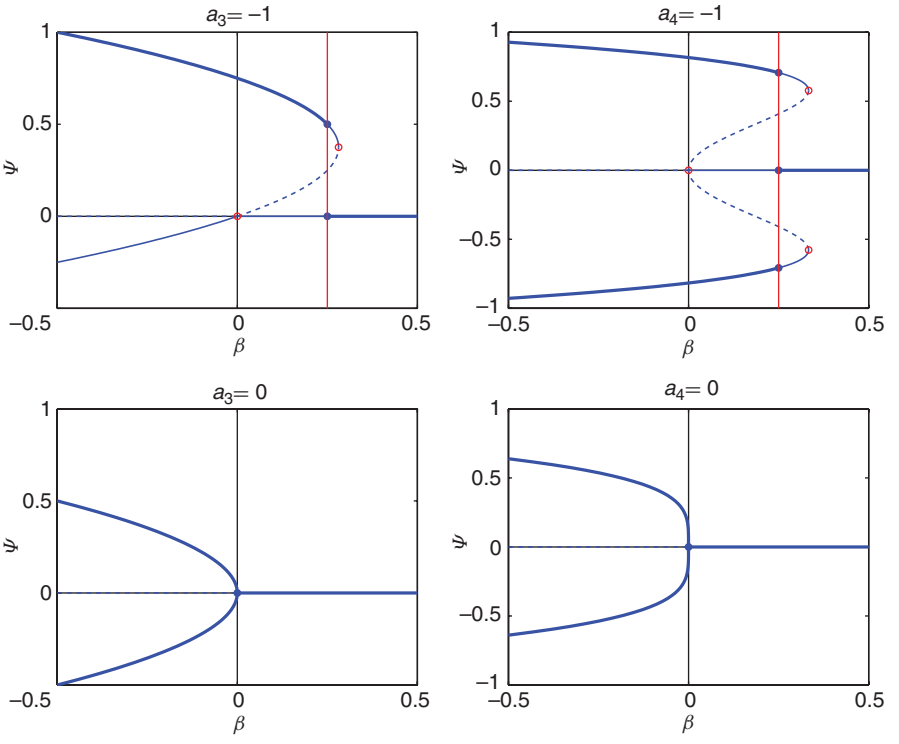

FIGURE 1. (Colour online) Model scenarios of transitions from first order to second order with *two* coalescing phases (left) versus *three* coalescing phases (right). Left: bifurcation diagram for model free energy $F_1(\psi) = \beta\psi^2 + a_3\psi^3 + \psi^4$ with $a_3 < 0$ (upper, first-order transition) versus $a_3 = 0$ (lower, second-order transition). Right: bifurcation for model free energy $F_2(\psi) = \beta\psi^2 + a_4\psi^4 + \psi^6$ with $a_4 < 0$ (upper, first order) versus $a_4 = 0$ (lower, second order). Dashed lines represent unstable equilibria; solid lines represent locally stable equilibria; heavy solid lines represent globally stable equilibria. The free-energy crossover point is indicated with a light vertical line, and the coexisting phases are indicated by heavy solid dots.

the uniaxial–biaxial transition in nematic liquid crystals treated in Section 4. Finally, in Section 5 we collect the main conclusions of this work and comment about their possible extension.

2 General setting

In this preliminary section, we present the general mathematical setting within which our bifurcation analysis of the equilibrium phases of an ordered condensate will be phrased.

Let $F : \mathbb{R}^{n+1} \to \mathbb{R}$ be a real-valued, smooth function representing either a mean-field free energy or a Landau potential that describes the different condensed ordered phases of a homogeneous system. We shall write $F = F(\boldsymbol{x}, \beta)$, where $\boldsymbol{x} = (x_1, \ldots, x_n) \in \mathbb{R}^n$ is the set of scalar order parameters and β is a parameter, typically a reciprocal dimensionless temperature. For a given value of β, the equilibrium condensed phases correspond to solutions of the equation

$$\boldsymbol{G}(\boldsymbol{x}, \beta) = \boldsymbol{0}, \tag{2.1}$$

https://doi.org/10.1017/S0956792510000355 Published online by Cambridge University Press

where

$$\boldsymbol{G}(\boldsymbol{x},\beta) := \nabla_{\boldsymbol{x}} F(\boldsymbol{x},\beta)\,.$$

We shall assume that (2.1) is solved by a special pair $(\boldsymbol{x}_0,\beta_0)$, with $\boldsymbol{x}_0 \in \mathbb{R}^n$ and $\beta_0 \in \mathbb{R}$. We are interested in any further solution to (2.1) in the vicinity of $(\boldsymbol{x}_0,\beta_0)$ that can be parameterised as $s \mapsto (\boldsymbol{x}(s),\beta(s))$, where s is a scalar parameter chosen in an open interval $I \subset \mathbb{R}$ containing 0, so that $\boldsymbol{x}(0) = \boldsymbol{x}_0$ and $\beta(0) = \beta_0$. Any such family $\mathscr{C} = (\boldsymbol{x}(s),\beta(s))$ will be called a *solution curve* of (2.1) based at $P_0 := (\boldsymbol{x}_0,\beta_0)$.

The function $\boldsymbol{G}$, restricted along a solution curve $\mathscr{C}$, becomes a function $\boldsymbol{\Gamma}$ of the parameter s that vanishes identically in I, that is,

$$\boldsymbol{\Gamma}(s) := \boldsymbol{G}(\boldsymbol{x}(s),\beta(s)) = \boldsymbol{0}\,, \quad \forall s \in I\,. \tag{2.2}$$

It further follows from (2.2) that

$$\dot{\boldsymbol{\Gamma}}(s) = \mathbf{H}(\boldsymbol{x}(s),\beta(s))\,\boldsymbol{t}(s) + \dot{\beta}(s)\,\boldsymbol{b}(\boldsymbol{x}(s),\beta(s)) = \boldsymbol{0}\,, \quad \forall s \in I\,, \tag{2.3}$$

where $\boldsymbol{t}(s) := \dot{\boldsymbol{x}}(s)$, the *Hessian* $\mathbf{H}$ of F is the symmetric tensor on $\mathbb{R}^n$ defined by

$$\mathbf{H}(\boldsymbol{x},\beta) := \nabla_{\boldsymbol{x}} \boldsymbol{G}(\boldsymbol{x},\beta) = \nabla^2_{\boldsymbol{x}} F(\boldsymbol{x},\beta) \tag{2.4}$$

and

$$\boldsymbol{b}(\boldsymbol{x},\beta) := \frac{\partial}{\partial\beta}\boldsymbol{G}(\boldsymbol{x},\beta) = \frac{\partial}{\partial\beta}\nabla_{\boldsymbol{x}} F(\boldsymbol{x},\beta)\,. \tag{2.5}$$

We say that P_0 is a *bifurcation point* whenever there are at least two solution curves of (2.1) based at P_0. Among all possible functions F, we shall consider in this paper only those that enjoy a certain symmetry, and among all possible bifurcation points only those where a solution curve of (2.1) is based that *breaks* such a symmetry. The particular symmetry we envisage here, relevant to symmetric tricritical points according to Griffith's definition [10, 11], is recalled in Section 2.1 together with the consequences it entails for our analysis.

2.1 $\mathbb{Z}_2$ symmetry

We collect some basic results for bifurcation problems that possess $\mathbb{Z}_2$ symmetry. We follow the developments in [8, 9 (ch. 8), 13].

We assume that our free-energy function F is invariant under a $\mathbb{Z}_2$ symmetry group. That is, we assume that there is an involution $\mathbf{S}$ on $\mathbb{R}^n$ that is orthogonal and symmetric (for involutions, one implies the other):

$$\mathbf{S}^2 = \mathbf{I}, \quad \mathbf{S}^{-1} = \mathbf{S}^{\mathsf{T}} = \mathbf{S}\,,$$

where $\mathbf{I}$ is the identity in $\mathbb{R}^n$. The group

$$\mathscr{S} = \{\mathbf{I}, \mathbf{S}\}$$

https://doi.org/10.1017/S0956792510000355 Published online by Cambridge University Press

is isomorphic to the group of integers modulo 2, and we assume that F is $\mathscr{S}$ *invariant*:

$$F(\mathbf{S}\boldsymbol{x},\beta) = F(\boldsymbol{x},\beta), \quad \forall \boldsymbol{x} \in \mathbb{R}^n,\ \forall \beta \in \mathbb{R}.$$

This symmetry induces an orthogonal decomposition of $\mathbb{R}^n$ into *symmetric* and *antisymmetric* subspaces:

$$\mathbb{R}^n = \mathbb{X}_\mathrm{s} \oplus \mathbb{X}_\mathrm{a}, \quad \mathbb{X}_\mathrm{s} \perp \mathbb{X}_\mathrm{a},$$

where

$$\mathbb{X}_\mathrm{s} := \{\boldsymbol{x} \in \mathbb{R}^n \,|\, \mathbf{S}\boldsymbol{x} = \boldsymbol{x}\}, \quad \mathbb{X}_\mathrm{a} := \{\boldsymbol{x} \in \mathbb{R}^n \,|\, \mathbf{S}\boldsymbol{x} = -\boldsymbol{x}\}.$$

Several consequences follow from the $\mathscr{S}$ invariance of F. Expansion around $\boldsymbol{y} = \mathbf{0}$ of both sides of the identity

$$F(\mathbf{S}\boldsymbol{x} + \boldsymbol{y},\beta) = F(\boldsymbol{x} + \mathbf{S}\boldsymbol{y},\beta),$$

using $\mathbf{S}^{-1} = \mathbf{S}^\mathsf{T} = \mathbf{S}$, gives

$$\nabla_{\boldsymbol{x}}^k F(\mathbf{S}\boldsymbol{x},\beta)\cdot(\boldsymbol{y}\otimes\cdots\otimes\boldsymbol{y}) = \nabla_{\boldsymbol{x}}^k F(\boldsymbol{x},\beta)\cdot(\mathbf{S}\boldsymbol{y}\otimes\cdots\otimes\mathbf{S}\boldsymbol{y}), \quad k = 1,2,\ldots. \tag{2.6}$$

The case $k = 1$ gives that the gradient is $\mathscr{S}$ *equivariant*:

$$\boldsymbol{G}(\mathbf{S}\boldsymbol{x},\beta) = \mathbf{S}\boldsymbol{G}(\boldsymbol{x},\beta), \quad \forall \boldsymbol{x} \in \mathbb{R}^n,\ \forall \beta \in \mathbb{R}.$$

Note also that for k *odd*, with $\boldsymbol{x} \in \mathbb{X}_\mathrm{s}$ (satisfying $\mathbf{S}\boldsymbol{x} = \boldsymbol{x}$) and $\boldsymbol{y} \in \mathbb{X}_\mathrm{a}$ (satisfying $\mathbf{S}\boldsymbol{y} = -\boldsymbol{y}$), (2.6) implies

$$\nabla_{\boldsymbol{x}}^k F(\boldsymbol{x},\beta)\cdot(\boldsymbol{y}\otimes\cdots\otimes\boldsymbol{y}) = 0,$$

from which follows

$$\nabla_{\boldsymbol{x}}^k F(\boldsymbol{x},\beta)\cdot(\boldsymbol{y}_1\otimes\cdots\otimes\boldsymbol{y}_k) = 0, \quad \forall \boldsymbol{x} \in \mathbb{X}_\mathrm{s},\ \forall \boldsymbol{y}_1,\ldots,\boldsymbol{y}_k \in \mathbb{X}_\mathrm{a},\ k = 1,3,5,\ldots \tag{2.7}$$

(since $\nabla_{\boldsymbol{x}}^k F$ is a symmetric multilinear form and as such is completely determined by its traces, or the so-called polar forms, $\nabla_{\boldsymbol{x}}^k F(\boldsymbol{x},\beta)\cdot(\boldsymbol{y}\otimes\cdots\otimes\boldsymbol{y})$ [2 (sec. 2.1)]). Again, the case $k = 1$ of the above gives

$$\boldsymbol{x} \in \mathbb{X}_\mathrm{s} \ \Rightarrow\ \boldsymbol{G}(\boldsymbol{x},\beta),\ \frac{\partial}{\partial\beta}\boldsymbol{G}(\boldsymbol{x},\beta),\ \ldots \in \mathbb{X}_\mathrm{s}.$$

In particular, the vector $\boldsymbol{b}$ defined in (2.5) satisfies

$$\boldsymbol{b}(\boldsymbol{x},\beta) \in \mathbb{X}_\mathrm{s}, \quad \forall \boldsymbol{x} \in \mathbb{X}_\mathrm{s}. \tag{2.8}$$

More generally, it follows from (2.7) that

$$\nabla_{\boldsymbol{x}}^k F(\boldsymbol{x},\beta)\cdot(\boldsymbol{y}_1\otimes\cdots\otimes\boldsymbol{y}_{k-1}) \in \mathbb{X}_\mathrm{s}, \quad \forall \boldsymbol{x} \in \mathbb{X}_\mathrm{s},\ \forall \boldsymbol{y}_1,\ldots,\boldsymbol{y}_{k-1} \in \mathbb{X}_\mathrm{a},\ k = 1,3,5,\ldots. \tag{2.9}$$

The case $k = 2$ of (2.6) yields

$$\mathbf{H}(\mathbf{S}\boldsymbol{x},\beta) = \mathbf{S}\mathbf{H}(\boldsymbol{x},\beta)\mathbf{S}, \quad \forall \boldsymbol{x} \in \mathbb{R}^n,\ \forall \beta \in \mathbb{R},$$

https://doi.org/10.1017/S0956792510000355 Published online by Cambridge University Press

where $\mathbf{H}$ is the Hessian, defined in (2.4). This implies that $\mathbb{X}_s$ and $\mathbb{X}_a$ are invariant subspaces of $\mathbf{H}(\boldsymbol{x},\beta)$ when $\mathbf{H}$ is evaluated at a point in the symmetric space:

$$\boldsymbol{x}\in\mathbb{X}_s \;\Rightarrow\; \mathbf{H}(\boldsymbol{x},\beta)\,\mathbb{X}_s\subset\mathbb{X}_s \quad\text{and}\quad \mathbf{H}(\boldsymbol{x},\beta)\,\mathbb{X}_a\subset\mathbb{X}_a.$$

This allows one to decompose the Hessian into symmetric and antisymmetric parts, when evaluated at a point $\boldsymbol{x}$ in $\mathbb{X}_s$:

$$\boldsymbol{x}\in\mathbb{X}_s \;\Rightarrow\; \mathbf{H}(\boldsymbol{x},\beta)=\mathbf{H}_s(\boldsymbol{x},\beta)+\mathbf{H}_a(\boldsymbol{x},\beta),\quad \mathbf{H}_s:=\mathbf{P}_s\mathbf{H}\mathbf{P}_s,\ \mathbf{H}_a:=\mathbf{P}_a\mathbf{H}\mathbf{P}_a, \tag{2.10}$$

where $\mathbf{P}_s$ is the orthogonal projection onto $\mathbb{X}_s$ and $\mathbf{P}_a=\mathbf{I}-\mathbf{P}_s$ is the orthogonal projection onto $\mathbb{X}_a$.

The invariance of $\mathbb{X}_s$ and $\mathbb{X}_a$ under $\mathbf{H}(\boldsymbol{x},\beta)$ for $\boldsymbol{x}\in\mathbb{X}_s$ has implications in terms of possible bifurcation scenarios. A solution curve in the symmetric space,

$$\boldsymbol{G}(\boldsymbol{x}(s),\beta(s))=\mathbf{0},\quad \boldsymbol{x}(s)\in\mathbb{X}_s,\ s\in I,$$

necessarily remains in the symmetric space unless it suffers a 'symmetry breaking bifurcation'. This is a consequence of the tangent-vector equation (2.3), which can be written at a point $(\boldsymbol{x}_0,\beta_0)$ as

$$\mathbf{H}_0\boldsymbol{t}_0+\dot\beta(0)\boldsymbol{b}_0=\mathbf{0}$$

with

$$\mathbf{H}_0:=\mathbf{H}(\boldsymbol{x}_0,\beta_0),\quad \boldsymbol{t}_0:=\dot{\boldsymbol{x}}(0),\quad \boldsymbol{b}_0:=\boldsymbol{b}(\boldsymbol{x}_0,\beta_0),$$

and the facts that, for $\boldsymbol{x}_0\in\mathbb{X}_s$, both $\mathbb{X}_s$ and $\mathbb{X}_a$ are invariant under $\mathbf{H}_0$ and $\boldsymbol{b}_0\in\mathbb{X}_s$.

A symmetry-breaking bifurcation point is a point $P_0=(\boldsymbol{x}_0,\beta_0)$ along a solution curve in $\mathbb{X}_s$ at which the tangent vector to a bifurcating branch satisfies

$$\boldsymbol{t}_0\in\mathbb{X}_a \text{ and necessarily } \dot\beta(0)=0. \tag{2.11}$$

This implies that $\mathbf{H}_a(\boldsymbol{x}_0,\beta_0)$ is singular and

$$\mathbb{K}\cap\mathbb{X}_a\neq\{\mathbf{0}\},\quad \text{where } \mathbb{K}:=\ker\mathbf{H}_0.$$

The situation is the cleanest when $\dim\mathbb{K}=1$. In this case, either $\mathbf{H}_s(\boldsymbol{x}_0,\beta_0)$ or $\mathbf{H}_a(\boldsymbol{x}_0,\beta_0)$ is singular (but not both). If $\mathbf{H}_s(\boldsymbol{x}_0,\beta_0)$ is singular, then the point P_0 could be either a limit point or a bifurcation point to another branch in $\mathbb{X}_s$. If $\mathbf{H}_a(\boldsymbol{x}_0,\beta_0)$ is singular, then the point is a potential symmetry-breaking bifurcation point, and the existence of a symmetry-breaking branch would be guaranteed by the 'Equivariant Branching Lemma', provided the necessary additional hypotheses are satisfied. See, for example, [8,9,13].

Exploring $\mathbb{K}$ and identifying the 'directions' $\boldsymbol{t}_0\in\mathbb{K}$ along which a symmetry-breaking bifurcation can take place is the essence of the general Lyapunov–Schmidt reduction method, amply illustrated, for example, in [7,8] (especially, in Secs. 1.3, 7.1 and 7.3 of the cited works). Here, such a general strategy will be adapted to our needs. To this end, we recall a number of preliminary results, which are collected in the remaining part of this section.

https://doi.org/10.1017/S0956792510000355 Published online by Cambridge University Press

At the $\mathbb{Z}_2$-symmetry-breaking bifurcation point, since $\mathbb{K}$ is non-trivial, and consequently $\boldsymbol{t}_0 \neq \mathbf{0}$, by continuity, it must also be $\dot{\boldsymbol{x}}(s) \neq \mathbf{0}$ in a neighbourhood of $s = 0$, which here we take as coincident with the whole of I. Thus, the parameter s can be chosen so as to be the *arc-length* along the bifurcating branch $\boldsymbol{x}(s)$ in $\mathbb{R}^n$. Such a choice will entail a few simplifications in what follows. Hereafter we shall denote by $\boldsymbol{t}(s)$ the *unit* vector tangent to the curve $\boldsymbol{x}(s)$:

$$\boldsymbol{t}(s) := \dot{\boldsymbol{x}}(s)\,,$$

which satisfies the condition

$$\boldsymbol{t}(s) \cdot \boldsymbol{t}(s) = 1\,, \quad \forall s \in I\,. \tag{2.12}$$

It follows immediately from (2.12) that

$$\ddot{\boldsymbol{x}}(s) \cdot \boldsymbol{t}(s) = 0\,, \quad \forall s \in I\,. \tag{2.13}$$

We shall assume that $\dim \mathbb{K} < n$. Moreover, we shall denote by $\mathbb{K}_\perp$ the orthogonal complement of $\mathbb{K}$ in $\mathbb{R}^n$, so that $\mathbb{R}^n$ can also be split as $\mathbb{R}^n = \mathbb{K} \oplus \mathbb{K}_\perp$. We further qualify as $\mathbb{K}$ *projection* the tensor $\mathbf{P}_{\mathbb{K}}$ that transforms any vector $\boldsymbol{v} \in \mathbb{R}^n$ into its component in $\mathbb{K}$; it can be represented as

$$\mathbf{P}_{\mathbb{K}} = \sum_{i=1}^{m} \boldsymbol{u}_i \otimes \boldsymbol{u}_i\,,$$

where $\{\boldsymbol{u}_1, \dots \boldsymbol{u}_m\}$ is any orthonormal basis for $\mathbb{K}$. Similarly, we define the $\mathbb{K}_\perp$ *projection* $\mathbf{P}_{\mathbb{K}_\perp}$ as

$$\mathbf{P}_{\mathbb{K}_\perp} := \mathbf{I} - \mathbf{P}_{\mathbb{K}}\,.$$

It is easily proved that

$$\mathbf{P}_{\mathbb{K}}\mathbf{H}_0 = \mathbf{H}_0\mathbf{P}_{\mathbb{K}} = \mathbf{0}\,.$$

Moreover, the restriction of $\mathbf{H}_0$ onto $\mathbb{K}_\perp$ can be inverted; we denote this restricted inversion as

$$\overline{\mathbf{H}_0^{-1}} := (\mathbf{H}_0|_{\mathbb{K}_\perp})^{-1}\,, \tag{2.14}$$

which is a tensor on $\mathbb{K}_\perp$, as $\overline{\mathbf{H}_0^{-1}}\,\mathbb{K}_\perp = \mathbb{K}_\perp$. We shall denote the projections delivered by $\mathbf{P}_{\mathbb{K}}$ and $\mathbf{P}_{\mathbb{K}_\perp}$, respectively, by $[\cdot]_{\mathbb{K}}$ and $[\cdot]_{\mathbb{K}_\perp}$. In particular, for any vector $\boldsymbol{v} \in \mathbb{R}^n$,

$$\boldsymbol{v}_{\mathbb{K}} := \mathbf{P}_{\mathbb{K}}\boldsymbol{v} \quad \text{and} \quad \boldsymbol{v}_{\mathbb{K}_\perp} := \mathbf{P}_{\mathbb{K}_\perp}\boldsymbol{v}\,.$$

It is worth remarking that although both $\mathbb{K}$ and $\mathbb{K}_\perp$ have here finite dimensions, the general Lyapunov–Schmidt reduction would also apply, were the dimension of $\mathbb{K}_\perp$ infinite.

3 Bifurcation equations

In this section we derive the equations that determine what solution curves $\mathscr{C} = (\boldsymbol{x}(s), \beta(s))$ can actually branch off a bifurcation point $P_0 = (\boldsymbol{x}_0, \beta_0)$ and break the $\mathbb{Z}_2$ symmetry enjoyed by $\boldsymbol{x}_0 \in \mathbb{X}_s$. Much in the original spirit of the Lyapunov–Schmidt method, presented in [28], also in its historical development (see [29], for a broader perspective), we perform an asymptotic expansion of $\mathscr{C}$ in the vicinity of P_0. Here this objective is

https://doi.org/10.1017/S0956792510000355 Published online by Cambridge University Press

pursued by successive differentiations of both sides of (2.3) with respect to s. We thus obtain the following equations:

$$\begin{aligned}\ddot{\boldsymbol{\Gamma}}(s) = {} & \nabla_{\boldsymbol{x}}^3 F(\boldsymbol{x}(s),\beta(s))\cdot[\dot{\boldsymbol{x}}(s)\otimes\dot{\boldsymbol{x}}(s)] + \nabla_{\boldsymbol{x}}^2 F(\boldsymbol{x}(s),\beta(s))\,\ddot{\boldsymbol{x}}(s)\\ & + 2\dot{\beta}(s)\frac{\partial}{\partial\beta}\nabla_{\boldsymbol{x}}^2 F(\boldsymbol{x}(s),\beta(s))\,\dot{\boldsymbol{x}}(s)\\ & + \ddot{\beta}(s)\frac{\partial}{\partial\beta}\nabla_{\boldsymbol{x}} F(\boldsymbol{x}(s),\beta(s)) + \dot{\beta}(s)^2\frac{\partial^2}{\partial\beta^2}\nabla_{\boldsymbol{x}} F(\boldsymbol{x}(s),\beta(s)) = \boldsymbol{0}\,,\quad \forall s\in I\,,\end{aligned} \tag{3.1}$$

and

$$\begin{aligned}\dddot{\boldsymbol{\Gamma}}(s) = {} & \nabla_{\boldsymbol{x}}^4 F(\boldsymbol{x}(s),\beta(s))\cdot[\dot{\boldsymbol{x}}(s)\otimes\dot{\boldsymbol{x}}(s)\otimes\dot{\boldsymbol{x}}(s)]\\ & + 3\nabla_{\boldsymbol{x}}^3 F(\boldsymbol{x}(s),\beta(s))\cdot[\dot{\boldsymbol{x}}(s)\otimes\ddot{\boldsymbol{x}}(s)] + \nabla_{\boldsymbol{x}}^2 F(\boldsymbol{x}(s),\beta(s))\,\dddot{\boldsymbol{x}}(s)\\ & + 3\dot{\beta}(s)\frac{\partial}{\partial\beta}\nabla_{\boldsymbol{x}}^3 F(\boldsymbol{x}(s),\beta(s))\cdot[\dot{\boldsymbol{x}}(s)\otimes\dot{\boldsymbol{x}}(s)] + 3\dot{\beta}(s)^2\frac{\partial^2}{\partial\beta^2}\nabla_{\boldsymbol{x}}^2 F(\boldsymbol{x}(s),\beta(s))\,\dot{\boldsymbol{x}}(s)\\ & + 3\frac{\partial}{\partial\beta}\nabla_{\boldsymbol{x}}^2 F(\boldsymbol{x}(s),\beta(s))\left[\ddot{\beta}(s)\dot{\boldsymbol{x}}(s) + \dot{\beta}(s)\ddot{\boldsymbol{x}}(s)\right] + 3\dot{\beta}(s)\ddot{\beta}(s)\frac{\partial^2}{\partial\beta^2}\nabla_{\boldsymbol{x}} F(\boldsymbol{x}(s),\beta(s))\\ & + \dot{\beta}(s)^3\frac{\partial^3}{\partial\beta^3}\nabla_{\boldsymbol{x}} F(\boldsymbol{x}(s),\beta(s)) + \dddot{\beta}(s)\frac{\partial}{\partial\beta}\nabla_{\boldsymbol{x}} F(\boldsymbol{x}(s),\beta(s)) = \boldsymbol{0}\,,\quad \forall s\in I\,.\end{aligned}$$

Both the above equations are then evaluated at $s=0$ by recalling that, by (2.11), $\dot{\beta}(0)=0$. By operating with the projection $\mathbf{P}_{\mathbb{K}}$ on both sides of the equations thus obtained and with the projection $\mathbf{P}_{\mathbb{K}_\perp}$ on both sides of the only equation obtained from (3.1), since $\mathbb{K}$ is invariant under $\mathbf{H}_0$, we finally arrive at

$$\left[\nabla_{\boldsymbol{x}}^3 F(\boldsymbol{x}_0,\beta_0)\cdot(\boldsymbol{t}_0\otimes\boldsymbol{t}_0)\right]_{\mathbb{K}} + \ddot{\beta}_0\boldsymbol{b}_{0\mathbb{K}} = \boldsymbol{0}\,, \tag{3.2a}$$

$$\left[\nabla_{\boldsymbol{x}}^3 F(\boldsymbol{x}_0,\beta_0)\cdot(\boldsymbol{t}_0\otimes\boldsymbol{t}_0)\right]_{\mathbb{K}_\perp} + \mathbf{H}_0\ddot{\boldsymbol{x}}_{0\mathbb{K}_\perp} + \ddot{\beta}_0\boldsymbol{b}_{0\mathbb{K}_\perp} = \boldsymbol{0}\,, \tag{3.2b}$$

$$\begin{aligned}\left[\nabla_{\boldsymbol{x}}^4 F(\boldsymbol{x}_0,\beta_0)\cdot(\boldsymbol{t}_0\otimes\boldsymbol{t}_0\otimes\boldsymbol{t}_0)\right]_{\mathbb{K}} & + 3\left[\nabla_{\boldsymbol{x}}^3 F(\boldsymbol{x}_0,\beta_0)\cdot(\ddot{\boldsymbol{x}}_0\otimes\boldsymbol{t}_0)\right]_{\mathbb{K}}\\ & + 3\ddot{\beta}_0\left[\mathbf{B}_0\boldsymbol{t}_0\right]_{\mathbb{K}} + \dddot{\beta}_0\boldsymbol{b}_{0\mathbb{K}} = \boldsymbol{0}\,,\end{aligned} \tag{3.2c}$$

where the subscript 0 denotes evaluation at $s=0$ and

$$\mathbf{B}_0 := \frac{\partial}{\partial\beta}\mathbf{H}(\boldsymbol{x}_0,\beta)\bigg|_{\beta=\beta_0}\,.$$

Hereafter we shall assume that

$$\mathbb{K}\subseteqq\mathbb{X}_{\mathrm{a}}\,, \tag{3.3}$$

so that only $\mathbf{H}_{\mathrm{a}}$ is singular at P_0. Such an assumption will considerably simplify our analysis, while encompassing the application envisaged in Section 4. It follows from (2.8) and (3.3) that $\boldsymbol{b}_{0\mathbb{K}}=\boldsymbol{0}$. Moreover, for $\boldsymbol{x}_0\in\mathbb{X}_{\mathrm{s}}$, (2.9) for $k=3$ implies that

$$\nabla_{\boldsymbol{x}}^3 F(\boldsymbol{x}_0,\beta_0)\cdot(\boldsymbol{t}_0\otimes\boldsymbol{t}_0)\in\mathbb{X}_{\mathrm{s}}\,, \tag{3.4}$$

whence it follows that

$$\left[\nabla_{\boldsymbol{x}}^3 F(\boldsymbol{x}_0,\beta_0)\cdot(\boldsymbol{t}_0\otimes\boldsymbol{t}_0)\right]_{\mathbb{K}} = \boldsymbol{0}\,, \tag{3.5}$$

https://doi.org/10.1017/S0956792510000355 Published online by Cambridge University Press

so that (3.2a) is identically satisfied. As already shown in (2.14), the Hessian $\mathbf{H}_0$ is invertible in $\mathbb{K}_\perp$, and so (3.2b) can be solved for $\ddot{\boldsymbol{x}}_{0\mathbb{K}_\perp}$:

$$\ddot{\boldsymbol{x}}_{0\mathbb{K}_\perp} = -\overline{\mathbf{H}_0^{-1}} \left(\nabla_{\boldsymbol{x}}^3 F(\boldsymbol{x}_0, \beta_0) \cdot (\boldsymbol{t}_0 \otimes \boldsymbol{t}_0) + \ddot{\beta}_0 \boldsymbol{b}_0 \right), \tag{3.6}$$

the projection onto $\mathbb{K}_\perp$ being omitted, again by (3.3) and (3.5). Furthermore, since $\boldsymbol{b}_0 \in \mathbb{X}_\mathrm{s}$, again by (3.4) we can give (3.6) the following equivalent form

$$\ddot{\boldsymbol{x}}_{0\mathbb{K}_\perp} = -\mathbf{H}_{0\mathrm{s}}^{-1} \left(\nabla_{\boldsymbol{x}}^3 F(\boldsymbol{x}_0, \beta_0) \cdot (\boldsymbol{t}_0 \otimes \boldsymbol{t}_0) + \ddot{\beta}_0 \boldsymbol{b}_0 \right), \tag{3.7}$$

where $\mathbf{H}_{0\mathrm{s}} := \mathbf{H}_\mathrm{s}(\boldsymbol{x}_0, \beta_0)$ is the non-singular component of $\mathbf{H}_0$ in the symmetric subspace $\mathbb{X}_\mathrm{s}$, defined as in (2.10). The vector $\ddot{\boldsymbol{x}}_0$ in (3.2c) can uniquely be decomposed as $\ddot{\boldsymbol{x}}_0 = \ddot{\boldsymbol{x}}_{0\mathbb{K}} + \ddot{\boldsymbol{x}}_{0\mathbb{K}_\perp}$, where $\ddot{\boldsymbol{x}}_{0\mathbb{K}} \in \mathbb{K}$ and $\ddot{\boldsymbol{x}}_{0\mathbb{K}_\perp} \in \mathbb{K}_\perp \cap \mathbb{X}_\mathrm{s} = \mathbb{X}_\mathrm{s}$. By (3.5), (3.2c) thus becomes

$$\left[\nabla_{\boldsymbol{x}}^4 F(\boldsymbol{x}_0, \beta_0) \cdot (\boldsymbol{t}_0 \otimes \boldsymbol{t}_0 \otimes \boldsymbol{t}_0) \right]_\mathbb{K} + 3 \left[\nabla_{\boldsymbol{x}}^3 F(\boldsymbol{x}_0, \beta_0) \cdot \left(\ddot{\boldsymbol{x}}_{0\mathbb{K}_\perp} \otimes \boldsymbol{t}_0 \right) \right]_\mathbb{K} + 3 \ddot{\beta}_0 \left[\mathbf{B}_0 \boldsymbol{t}_0 \right]_\mathbb{K} = \mathbf{0}, \tag{3.8}$$

where $\ddot{\boldsymbol{x}}_{0\mathbb{K}_\perp}$ is given by (3.7).

While $\ddot{\boldsymbol{x}}_{0\mathbb{K}_\perp}$ is determined by (3.7), determining $\ddot{\boldsymbol{x}}_{0\mathbb{K}}$ would in general require deriving higher order asymptotic equations – computing $\dddot{\boldsymbol{\Gamma}}(s)$ and possibly higher derivatives of the function $\boldsymbol{\Gamma}(s)$ in (2.2), except in the case where $\dim \mathbb{K} = 1$, as in this case $\ddot{\boldsymbol{x}}_{0\mathbb{K}} = \mathbf{0}$, by (2.13) evaluated at $s = 0$. As will be seen below, the case $\dim \mathbb{K} = 1$ is remarkably simpler: for it our analysis also becomes more stringent. Equation (3.8) is the general vector form of the bifurcation equation in the unknowns $(\boldsymbol{t}_0, \ddot{\beta}_0)$ for a reflectional symmetry breaking. It is clear from its structure that its solutions come in reflectional symmetric pairs: any solution $(\boldsymbol{t}_0, \ddot{\beta}_0)$ is accompanied by $(-\boldsymbol{t}_0, \ddot{\beta}_0)$, each solution representing a 'half-branch' emanating from $\boldsymbol{x}_0 \in \mathbb{X}_\mathrm{s}$ into $\mathbb{X}_\mathrm{a}$.

Equation (3.8) can be reduced to a system of m scalar equations, linear in $\ddot{\beta}_0$ and cubic in the $m-1$ independent scalar components u_i of $\boldsymbol{t}_0$ in a basis $\{\boldsymbol{u}_1, \ldots, \boldsymbol{u}_m\}$ of $\mathbb{K}$, where $m = \dim \mathbb{K}$. Such a system of algebraic equations will be easily solved in Section 3.1.1 for $\dim \mathbb{K} = 1$, a case relevant to our application in Section 4. Here we remark that in general they are but a set of compatibility conditions and there is no guarantee that a solution to the scalar bifurcation equations corresponds indeed to a solution curve $\mathscr{C}$ for the equilibrium equation (2.1). Different existence theorems that fill this gap have been provided in the literature under different analytical assumptions, such as Theorem 4.1 in [28] (see, in particular, Claim 3) and Theorem 4.12 in [14], just to quote two among the earliest contributions to the bifurcation theory. Here we do not dwell further on this issue. As customary in many applied studies, we assume that a pair $(\boldsymbol{t}_0, \ddot{\beta}_0)$ that solves (3.8) identifies the lowest order in an asymptotic expansion near P_0 of a bifurcated solution that breaks a reflectional symmetry. This is in keeping with the numerical approach followed in Section 4, where the solutions to the algebraic bifurcation equations drive a continuation algorithm.

3.1 Tricriticality criterion

As explained in the Introduction, according to the definition we have adopted, a tricritical point occurs wherever in a phase diagram a phase transition changes from first to second

https://doi.org/10.1017/S0956792510000355 Published online by Cambridge University Press

order as a control parameter, typically related to the temperature, is changed. Thus, by its own nature, a tricritical point is connected to a global property of the potential F. If, for example, F represents the mean-field approximation to the free energy of an ordering physical system, the stable equilibrium phase at a given value of β is represented by the set of stationary points $\{\boldsymbol{x}_{\mathrm{m}}(\beta)\}$ of $F(\cdot,\beta)$ where F attains its least value. As shown in [5], this minimum principle also applies to the case where F is *indefinite*, and thus possesses neither a global minimum nor a global maximum. Our local bifurcation analysis can become predictive of the occurrence of a tricritical point in the equilibrium phase diagram of the physical system described by F only in the light of extra information on the global behaviour of F. Generally, such information stems from the knowledge of the *ground state* of F, defined as the class of symmetry-related equilibrium configurations $\{\boldsymbol{x}_\infty\}$ with the least value of F in the asymptotic limit as the absolute temperature approaches zero: under appropriate regularity assumptions, $\{\boldsymbol{x}_\infty\} = \lim_{\beta\to\infty}\{\boldsymbol{x}_{\mathrm{m}}(\beta)\}$. Relating the symmetry enjoyed by the ground state of F to the symmetry of the molecular interactions – often known *a priori* – that concur to a microscopic definition of F is, to our knowledge, still an open problem. Here we assume that the ground state of F possesses the $\mathbb{Z}_2$ symmetry broken by the bifurcation being considered and that the symmetry-breaking bifurcating branch approaches an equilibrium configuration in $\{\boldsymbol{x}_\infty\}$ as $\beta \to \infty$.

With such an assumption of a global nature, distinguishing between putative first- and second-order transitions becomes an issue that can be resolved locally. In particular, if $\ddot{\beta}_0 > 0$ at the bifurcation point $P_0 = (\boldsymbol{x}_0, \beta_0)$, that is, if the bifurcation is *supercritical* in β, being $\dot{\beta}_0 = 0$, the corresponding transition is likely to be of second order, as no equilibrium state close to $\boldsymbol{x}_0$ could be found for $\beta < \beta_0$ along the bifurcating branch. Contrariwise, if $\ddot{\beta}_0 < 0$, that is, if the bifurcation is *subcritical* in β, the transition is likely to be of first order. (This is the situation depicted on the right panels of Figure 1, which also serve here as models for our discussion). Clearly, even in the light of our global assumption, relating supercritical and subcritical bifurcations to second- and first-order transitions remains conjectural, in the absence of a stability analysis of the bifurcating branch. Here we start by adopting the vanishing of $\ddot{\beta}_0$ as a criterion to signal a possible tricritical point; it will be corroborated by the stability analysis performed in Section 3.2.

3.1.1 *Case* $\dim \mathbb{K} = 1$

In the case where $\dim \mathbb{K} = 1$, the unit vector $\boldsymbol{t}_0$ is determined within its sign by merely being a non-trivial member of $\mathbb{K}$. Equation (3.8) thus reduces to a scalar equation for $\ddot{\beta}_0$, which is easily given the following linear form:

$$3\xi\ddot{\beta}_0 - \tau = 0\,, \tag{3.9}$$

where

$$\xi := \boldsymbol{t}_0 \cdot \left[\nabla^3_{\boldsymbol{x}} F(\boldsymbol{x}_0,\beta_0)\cdot\left(\mathbf{H}_{0\mathrm{s}}^{-1}\boldsymbol{b}_0\otimes\boldsymbol{t}_0\right) - \mathbf{B}_0\boldsymbol{t}_0\right] \tag{3.10}$$

and

$$\begin{aligned}\tau := {} & \nabla^4_{\boldsymbol{x}} F(\boldsymbol{x}_0,\beta_0)\cdot(\boldsymbol{t}_0\otimes\boldsymbol{t}_0\otimes\boldsymbol{t}_0\otimes\boldsymbol{t}_0)\\ & -3\nabla^3_{\boldsymbol{x}} F(\boldsymbol{x}_0,\beta_0)\cdot\left(\mathbf{H}_{0\mathrm{s}}^{-1}[\nabla^3_{\boldsymbol{x}} F(\boldsymbol{x}_0,\beta_0)\cdot(\boldsymbol{t}_0\otimes\boldsymbol{t}_0)]\otimes\boldsymbol{t}_0\otimes\boldsymbol{t}_0\right).\end{aligned} \tag{3.11}$$

https://doi.org/10.1017/S0956792510000355 Published online by Cambridge University Press

Clearly, if $\xi = 0$, the bifurcation equation (3.9) is compatible only if $\tau = 0$, but it fails to determine $\ddot{\beta}_0$. If, on the contrary, $\xi \neq 0$, (3.9) determines $\ddot{\beta}_0$, and this vanishes whenever τ does. Thus, for $\dim \mathbb{K} = 1$, if $\xi \neq 0$, our tricriticality criterion simply reads as $\tau = 0$.

3.2 Stability analysis

Here we study the stability of the bifurcating branch in the vicinity of the bifurcation point, P_0. Such a study relies on the evaluation of the eigenvalues of the Hessian $\mathbf{H}(\boldsymbol{x}(s), \beta(s))$ for s near 0. Clearly, for $s = 0$, $\mathbf{H}_0$ possesses the eigenvalue, $\lambda_0 = 0$, with multiplicity $m = \dim \mathbb{K}$. We are interested in evaluating the sign of the m eigenvalues of $\mathbf{H}(\boldsymbol{x}(s), \beta(s))$ that are close to nought as s grows away from $s = 0$, the sign of all others remaining unchanged by continuity.

For ε sufficiently small, a solution curve $\mathscr{C}_\varepsilon = (\boldsymbol{x}_\varepsilon, \beta_\varepsilon)$ in the vicinity of P_0 is represented through the following asymptotic expansions:

$$\boldsymbol{x}_\varepsilon := \boldsymbol{x}(\varepsilon) = \boldsymbol{x}_0 + \varepsilon\, \boldsymbol{t}_0 + \frac{1}{2}\varepsilon^2 \ddot{\boldsymbol{x}}_0 + o(\varepsilon^2), \tag{3.12a}$$

$$\beta_\varepsilon := \beta(\varepsilon) = \beta_0 + \frac{1}{2}\varepsilon^2 \ddot{\beta}_0 + o(\varepsilon^2), \tag{3.12b}$$

where the pair $(\boldsymbol{t}_0, \ddot{\beta}_0)$ solves the bifurcation equation (3.8). Let $\boldsymbol{u}_\varepsilon$ be any eigenvector of $\mathbf{H}_\varepsilon := \mathbf{H}(\boldsymbol{x}_\varepsilon, \beta_\varepsilon)$ with eigenvalue λ_ε approaching $\lambda_0 = 0$ as $\varepsilon \to 0$, so that

$$\mathbf{H}_\varepsilon \boldsymbol{u}_\varepsilon = \lambda_\varepsilon \boldsymbol{u}_\varepsilon . \tag{3.13}$$

Paralleling (3.12), we represent λ_ε and $\boldsymbol{u}_\varepsilon$ as

$$\lambda_\varepsilon = \varepsilon \dot{\lambda}_0 + \frac{1}{2}\varepsilon^2 \ddot{\lambda}_0 + o(\varepsilon^2), \tag{3.14a}$$

$$\boldsymbol{u}_\varepsilon = \boldsymbol{u}_0 + \varepsilon\, \dot{\boldsymbol{u}}_0 + \frac{1}{2}\varepsilon^2 \ddot{\boldsymbol{u}}_0 + o(\varepsilon^2), \tag{3.14b}$$

where $\dot{\boldsymbol{u}}_0 \cdot \boldsymbol{u}_0 = 0$ and

$$\ddot{\boldsymbol{u}}_0 \cdot \boldsymbol{u}_0 = -\dot{\boldsymbol{u}}_0 \cdot \dot{\boldsymbol{u}}_0 \tag{3.15}$$

to guarantee that $\boldsymbol{u}_\varepsilon \cdot \boldsymbol{u}_\varepsilon = 1$, up to second order in ε. For ε sufficiently small, $\boldsymbol{u}_\varepsilon$ is close to $\mathbb{K}$, and $\boldsymbol{u}_0 \in \mathbb{K}$. The asymptotic expansions in (3.14) are unknown, and our objective here is to derive equations that are able to determine them.

By expanding $\mathbf{H}_\varepsilon$ up to the second order in ε, with the aid of (3.12), we readily arrive at

$$\begin{aligned} \mathbf{H}_\varepsilon = \mathbf{H}_0 &+ \varepsilon \nabla^3_{\boldsymbol{x}} F(x_0, \beta_0) \cdot \boldsymbol{t}_0 \\ &+ \frac{1}{2}\varepsilon^2 \big(\nabla^3_{\boldsymbol{x}} F(x_0, \beta_0) \cdot \ddot{\boldsymbol{x}}_0 + \ddot{\beta}_0 \mathbf{B}_0 + \nabla^4_{\boldsymbol{x}} F(x_0, \beta_0) \cdot (\boldsymbol{t}_0 \otimes \boldsymbol{t}_0) \big) + o(\varepsilon^2). \end{aligned} \tag{3.16}$$

https://doi.org/10.1017/S0956792510000355 Published online by Cambridge University Press

It easily follows from (3.14) and (3.16) that (3.13) can be given the form

$$\begin{aligned}
&\varepsilon\left(\nabla_{\boldsymbol{x}}^3 F(\boldsymbol{x}_0,\beta_0)\cdot(\boldsymbol{t}_0\otimes\boldsymbol{u}_0)+\mathbf{H}_0\dot{\boldsymbol{u}}_0\right)\\
&\quad+\frac{1}{2}\varepsilon^2\big(\ddot{\beta}_0\mathbf{B}_0\boldsymbol{u}_0+\nabla_{\boldsymbol{x}}^4 F(\boldsymbol{x}_0,\beta_0)\cdot(\boldsymbol{t}_0\otimes\boldsymbol{t}_0\otimes\boldsymbol{u}_0)\\
&\quad+\nabla_{\boldsymbol{x}}^3 F(\boldsymbol{x}_0,\beta_0)\cdot(\ddot{\boldsymbol{x}}_0\otimes\boldsymbol{u}_0)+2\nabla_{\boldsymbol{x}}^3 F(\boldsymbol{x}_0,\beta_0)\cdot(\boldsymbol{t}_0\otimes\dot{\boldsymbol{u}}_0)+\mathbf{H}_0\ddot{\boldsymbol{u}}_0\big)\\
&=\varepsilon\dot{\lambda}_0\boldsymbol{u}_0+\frac{1}{2}\varepsilon^2\big(\ddot{\lambda}_0\boldsymbol{u}_0+2\dot{\lambda}_0\dot{\boldsymbol{u}}_0\big)+o(\varepsilon^2)\,.
\end{aligned}$$

By requiring this equation to be satisfied up to second order in ε, we conclude that

$$\mathbf{H}_0\dot{\boldsymbol{u}}_0+\nabla_{\boldsymbol{x}}^3 F(\boldsymbol{x}_0,\beta_0)\cdot(\boldsymbol{t}_0\otimes\boldsymbol{u}_0)=\dot{\lambda}_0\boldsymbol{u}_0\,, \tag{3.17a}$$

$$\begin{aligned}
&\nabla_{\boldsymbol{x}}^4 F(\boldsymbol{x}_0,\beta_0)\cdot(\boldsymbol{t}_0\otimes\boldsymbol{t}_0\otimes\boldsymbol{u}_0)+\nabla_{\boldsymbol{x}}^3 F(\boldsymbol{x}_0,\beta_0)\cdot(\ddot{\boldsymbol{x}}_0\otimes\boldsymbol{u}_0)\\
&+2\nabla_{\boldsymbol{x}}^3 F(\boldsymbol{x}_0,\beta_0)\cdot(\boldsymbol{t}_0\otimes\dot{\boldsymbol{u}}_0)+\ddot{\beta}_0\mathbf{B}_0\boldsymbol{u}_0+\mathbf{H}_0\ddot{\boldsymbol{u}}_0=\ddot{\lambda}_0\boldsymbol{u}_0+2\dot{\lambda}_0\dot{\boldsymbol{u}}_0\,.
\end{aligned} \tag{3.17b}$$

By (3.5), since $\boldsymbol{u}_0\in\mathbb{K}$, projecting both sides of (3.17a) along $\boldsymbol{u}_0$, one finds that

$$\dot{\lambda}_0=0\,. \tag{3.18}$$

Thus the sign of λ_ε is established at the second order in ε, and it is clearly the same for both half-branches, as reversing the sign of ε amounts to reversing $\boldsymbol{t}_0$. By decomposing $\dot{\boldsymbol{u}}_0$ as $\dot{\boldsymbol{u}}_0=\dot{\boldsymbol{u}}_{0\mathbb{K}}+\dot{\boldsymbol{u}}_{0\mathbb{K}_\perp}$, we, from (3.17a) and (3.18), easily obtain

$$\dot{\boldsymbol{u}}_{0\mathbb{K}_\perp}=-\mathbf{H}_{s0}^{-1}\left(\nabla_{\boldsymbol{x}}^3 F(\boldsymbol{x}_0,\beta_0)\cdot(\boldsymbol{t}_0\otimes\boldsymbol{u}_0)\right), \tag{3.19}$$

where use has been made again of (2.9) for $k=3$. Since both $\dot{\boldsymbol{u}}_{0\mathbb{K}}$ and $\ddot{\boldsymbol{x}}_{0\mathbb{K}}$ enter (3.17b) and at the present order of asymptotic approximation they remain undetermined, (3.17b) cannot be reduced into an equation for $\boldsymbol{u}_0$ only, except in the case where $\dim\mathbb{K}=1$, which entails that both $\dot{\boldsymbol{u}}_{0\mathbb{K}}$ and $\ddot{\boldsymbol{x}}_{0\mathbb{K}}$ vanish. This case again deserves a separate treatment.

3.2.1 *Case* $\dim\mathbb{K}=1$

For $\dim\mathbb{K}=1$, $\boldsymbol{u}_0$ is parallel to $\boldsymbol{t}_0$, and with no loss of generality we can take $\boldsymbol{u}_0=\boldsymbol{t}_0$. Now, the right-hand side of (3.19) delivers indeed $\dot{\boldsymbol{u}}_0$ as does the right-hand side of (3.7) for $\ddot{\boldsymbol{x}}_0$; comparing these equations, one finds that

$$\dot{\boldsymbol{u}}_0=\ddot{\boldsymbol{x}}_0+\ddot{\beta}_0\mathbf{H}_{s0}^{-1}\boldsymbol{b}_0\,. \tag{3.20}$$

On the other hand, projecting both sides of (3.17b) along $\boldsymbol{u}_0$, by (3.18) one easily arrives at

$$\begin{aligned}
\ddot{\lambda}_0=&\nabla_{\boldsymbol{x}}^4 F(\boldsymbol{x}_0,\beta_0)\cdot(\boldsymbol{t}_0\otimes\boldsymbol{t}_0\otimes\boldsymbol{t}_0\otimes\boldsymbol{t}_0)+\nabla_{\boldsymbol{x}}^3 F(\boldsymbol{x}_0,\beta_0)\cdot(\ddot{\boldsymbol{x}}_0\otimes\boldsymbol{t}_0\otimes\boldsymbol{t}_0)\\
&+2\nabla_{\boldsymbol{x}}^3 F(\boldsymbol{x}_0,\beta_0)\cdot(\dot{\boldsymbol{u}}_0\otimes\boldsymbol{t}_0\otimes\boldsymbol{t}_0)+\ddot{\beta}_0\mathbf{B}_0\boldsymbol{t}_0\cdot\boldsymbol{t}_0\,.
\end{aligned} \tag{3.21}$$

By further inserting both (3.20) and (3.7) into (3.21), also with the aid of (3.10) and (3.11), we finally obtain

$$\ddot{\lambda}_0=\tau-\xi\ddot{\beta}_0=\frac{2}{3}\tau\,, \tag{3.22}$$

https://doi.org/10.1017/S0956792510000355 Published online by Cambridge University Press

where (3.9) has been used. By projecting both sides of (3.17b) onto $\mathbb{K}_\perp$, we easily determine $\ddot{\boldsymbol{u}}_{0\mathbb{K}_\perp}$, while $\ddot{\boldsymbol{u}}_{0\mathbb{K}}$ is determined by (3.15).

Equations (3.22) and (3.18) show that when $\dim \mathbb{K} = 1$, the sign of τ is the same as that of the eigenvalue λ_ε of $\mathbf{H}_\varepsilon$ that vanishes for $\varepsilon = 0$. A positive λ_ε qualifies a stable branch, and this also applies to the class of indefinite free energies F studied in [5]. It was indeed shown there that for an equilibrium phase the number of negative eigenvalues of $\mathbf{H}$ cannot be less than a 'repulsive dimension' characteristic of the microscopic interaction potential: if an eigenvalue λ_0 of $\mathbf{H}$ vanishes at a bifurcation point, thus jeopardising the stability of an equilibrium phase, then stability can be restored along a bifurcating branch if $\ddot{\lambda}_0 > 0$.

We are now in a position to quantitatively interpret the scenarios illustrated on the right panels of Figure 1. By (3.22), a first-order transition occurs whenever *both* $\ddot{\beta}_0$ and τ are negative; contrariwise, a second-order transition occurs whenever both $\ddot{\beta}_0$ and τ are positive. We immediately see that the either case requires $\ddot{\beta}_0 \tau > 0$. Assuming that $\xi \neq 0$, by (3.9) we reduce the latter inequality to $\xi > 0$, which thus characterises the scenarios depicted in the right panels of Figure 1. We conclude that for $\dim \mathbb{K} = 1$ a phase transition is likely to be

$$\textit{first order} \text{ for } \xi > 0 \text{ and } \tau < 0\,, \text{ and } \textit{second order} \text{ for } \xi > 0 \text{ and } \tau > 0\,. \tag{3.23}$$

A tricritical point may then arise whenever $\xi > 0$ and $\tau = 0$, strengthening the criterion already envisaged above. Such a criterion extends to the case of an arbitrary number of scalar order parameters, the one derived in [4], with a different method, for the condensed phases described by two scalar order parameters. In the following section we apply the criterion derived here to a system with four scalar order parameters.

4 Symmetric tricritical points in biaxial nematics

The results of the previous sections have been used in the analysis of a certain mean-field model for biaxial nematic liquid crystals. The simplest (and most common) liquid-crystal fluid phase is the *uniaxial* nematic phase, which manifests long-range orientational order of a distinguished molecular axis but no positional order in the centres of mass of the molecules. In contrast, the *biaxial* nematic phase comprises some degree of orientational order with respect to *two* molecular axes.

The existence of a bulk biaxial nematic phase was first demonstrated for lyotropic liquid crystals (solutions) by Yu and Saupe in 1980 [32]. Only recently, and after years of effort, has the phase been realised in thermotropic liquid crystals (homogeneous systems) – see, for example, [20] and references therein. These materials are currently of high interest from the basic scientific point of view and also because of their potential for technological applications. This has led in turn to a high interest in mathematical models for biaxial nematics.

Mean-field models are simplified, approximate models for the collective behaviour of extremely large ensembles of interacting particles. These are derived in systematic ways by replacing the details of the interactions that a single particle has with the rest of the particles in an ensemble by the interaction with a single 'mean field' felt by the particle

https://doi.org/10.1017/S0956792510000355 Published online by Cambridge University Press

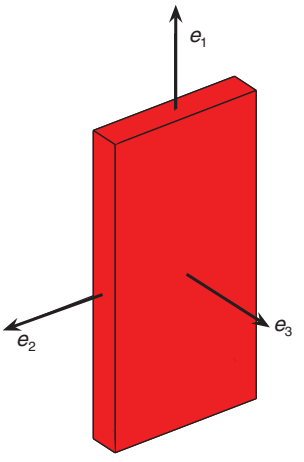

FIGURE 2. (Colour online) Idealised molecular architecture for particles forming a biaxial nematic phase.

(and to which the particle itself also contributes). Mean-field models are valuable tools for analysing the qualitative behaviour of bulk systems.

In the area of liquid crystals, the most famous mean-field model is that of Maier and Saupe [21, 22], which successfully predicts the weak first-order nature of the isotropic-uniaxial phase transition. A mean-field model for the biaxial nematic phase was proposed by Straley in 1974 [26] and reconsidered by Sonnet, Virga and Durand in 2003 [25]. The bifurcation and phase behaviour of this model has been explored in a series of papers culminating in [1]. The phase diagram involves three states of the system, isotropic, uniaxial nematic and biaxial nematic, which exist in different ranges of temperature and for different values of material parameters, and it contains both first-order and second-order transitions, as well as triple points and tricritical points. The tricriticality criterion developed in the previous section has been used to identify candidate symmetric tricritical points. Here we discuss its implementation in the context of this model.

4.1 The model

Straley's mean-field model for biaxial nematics begins from a *pair potential* or the *two-particle Hamiltonian* for the interaction of two particles whose idealised molecular architecture is that of a platelet, as in Figure 2. The orientational pair potential is a function of only the relative orientation of two such particles, the dependence on intermolecular separation having been removed by averaging. We let Ω denote the set of all possible orientations of a particle with respect to some fixed frame of reference. An orientation $\omega \in \Omega$ can be expressed in several ways, e.g. in terms of molecular frame vectors $(\boldsymbol{e}_1, \boldsymbol{e}_2, \boldsymbol{e}_3)$, Euler angles (θ, ϕ, ψ), rotation matrices $\mathsf{R} \in SO(3)$ etc. Given two orientations, $\omega, \omega' \in \Omega$, the two-particle Hamiltonian associates a potential energy to their relative orientation.

Straley's model pair potential is most cleanly expressed model in terms of contractions of real, symmetric and traceless tensors that are built from the frame vectors of the two interacting particles and are invariant under the symmetry of the platelet geometry,

https://doi.org/10.1017/S0956792510000355 Published online by Cambridge University Press

$\boldsymbol{e}_i \leftrightarrow -\boldsymbol{e}_i$, $i = 1, 2, 3$:

$$\begin{aligned} H(\omega, \omega') &= -U_0[\mathbf{q} \cdot \mathbf{q}' + \gamma(\mathbf{q} \cdot \mathbf{b}' + \mathbf{b} \cdot \mathbf{q}') + \lambda \mathbf{b} \cdot \mathbf{b}'] \\ \mathbf{q}(\omega) &:= \boldsymbol{e}_1(\omega) \otimes \boldsymbol{e}_1(\omega) - \frac{1}{3}\mathbf{I}, \quad \mathbf{b}(\omega) := \boldsymbol{e}_2(\omega) \otimes \boldsymbol{e}_2(\omega) - \boldsymbol{e}_3(\omega) \otimes \boldsymbol{e}_3(\omega). \end{aligned} \tag{4.1}$$

The function H can be viewed as a reduction of a more general expansion, truncated at quadrupolar order [19, 25]. Here U_0 represents a positive interaction energy. For values of the dimensionless material parameters γ and λ in an appropriate range [1, 3], $H(\omega, \omega')$ will achieve its minimum values when the two frames are aligned: $\boldsymbol{e}_i \parallel \boldsymbol{e}_i'$, $i = 1, 2, 3$. Thus, the nature of the interaction model is to encourage such an alignment.

The orientational Hamiltonian for an ensemble of identical particles interacting through such a potential is simply the sum over all pairwise interactions:

$$\mathscr{H}(\boldsymbol{\omega}) = \sum_{i<j} H(\omega_i, \omega_j), \quad \boldsymbol{\omega} = (\omega_1, \ldots, \omega_N) \in \Omega^N.$$

The equilibrium orientational probability density function follows the Boltzmann distribution with normalisation constant given by the ensemble *partition function*:

$$\begin{aligned} \rho(\boldsymbol{\omega}, \beta) &= \frac{e^{-\beta \mathscr{H}(\boldsymbol{\omega})}}{\mathscr{Z}(\beta)}, \quad \mathscr{Z}(\beta) = \int_{\Omega^N} e^{-\beta \mathscr{H}(\boldsymbol{\omega})} \mathrm{d}\boldsymbol{\omega}, \quad \beta := \frac{1}{k_B t} \\ d\boldsymbol{\omega} &= d\omega_1 \cdots d\omega_N, \quad d\omega_i = \sin\theta_i \, d\theta_i \, d\phi_i \, d\psi_i, \ i = 1, \ldots, N. \end{aligned}$$

Here k_B is the Boltzmann constant, and t is absolute temperature. Ensemble averages are denoted as

$$\langle g \rangle_\rho := \int_{\Omega^N} g(\boldsymbol{\omega}) \rho(\boldsymbol{\omega}, \beta) \, d\boldsymbol{\omega},$$

and the free energy of the ensemble is given by

$$\mathscr{F}(\beta) = -\frac{1}{\beta} \ln \mathscr{Z}(\beta).$$

See, for example, [5] and references contained therein.

The mean-field approximation to the ensemble free energy above is most cleanly expressed in tensorial form, while it is necessary to use scalar variables and orientation angles to work with it numerically. It begins by replacing the two-particle Hamiltonian with a single-particle potential of interaction between a particle and the 'mean field' generated by the ensemble:

$$H_0(\omega) = z\left[\langle H(\omega, \cdot) \rangle_{\rho_0} - \frac{1}{2} \langle H(\cdot, \cdot) \rangle_{\rho_0^2}\right].$$

Here the scaling factor z is the average number of interactions per particle ($N(N-1)/2$, if all particles interact), and the constant $\frac{1}{2}\langle H \rangle$ must be subtracted to avoid the overcounting that would result without it when summing over the ensemble. From Straley's pair

https://doi.org/10.1017/S0956792510000355 Published online by Cambridge University Press

potential (4.1), one obtains the single-particle Hamiltonian as

$$\frac{1}{zU_0}H_0(\omega;\mathbf{Q},\mathbf{B}) = \frac{1}{2}(\mathbf{Q}\cdot\mathbf{Q} + 2\gamma\,\mathbf{Q}\cdot\mathbf{B} + \lambda\,\mathbf{B}\cdot\mathbf{B}) \\ - \{\mathbf{q}(\omega)\cdot\mathbf{Q} + \gamma[\mathbf{q}(\omega)\cdot\mathbf{B} + \mathbf{b}(\omega)\cdot\mathbf{Q}] + \lambda\mathbf{b}(\omega)\cdot\mathbf{B}\},$$

where

$$\mathbf{Q} = \langle\mathbf{q}(\cdot)\rangle_{\rho_0}, \quad \mathbf{B} = \langle\mathbf{b}(\cdot)\rangle_{\rho_0}. \tag{4.2}$$

The tensors $\mathbf{Q}$ and $\mathbf{B}$ above represent the mean field and are referred to as 'order tensors'. These are equal to the zero tensor in the isotropic, disordered state (when ρ_0 is the uniform probability density). A non-zero value of either $\mathbf{Q}$ or $\mathbf{B}$ indicates some degree of order in the system. The mean-field equilibrium orientational probability distribution function again follows the Boltzmann law, normalised by the mean-field partition function:

$$\rho_0(\omega,\beta,\mathbf{Q},\mathbf{B}) = \frac{e^{-\beta H_0(\omega,\mathbf{Q},\mathbf{B})}}{Z_0(\beta,\mathbf{Q},\mathbf{B})}, \quad Z_0(\beta,\mathbf{Q},\mathbf{B}) = \int_\Omega e^{-\beta H_0(\omega,\mathbf{Q},\mathbf{B})}d\omega\,.$$

Note that the mean-field model of the orientational state depends on the order tensors $\mathbf{Q}$ and $\mathbf{B}$ and that the defining equations (4.2) are in fact *implicit*, as the probability distribution function with respect to which the averages are being calculated itself depends on $\mathbf{Q}$ and $\mathbf{B}$. For this reason, equations (4.2) are referred to as 'self-consistency' equations, and the mean-field models are sometimes referred to as 'self-consistent field theories'.

The mean-field approximation to the free energy of the ensemble (per particle) is given by

$$F_0(\beta,\mathbf{Q},\mathbf{B}) = -\frac{1}{\beta}\ln Z_0(\beta,\mathbf{Q},\mathbf{B})\,.$$

For Straley's model, in dimensionless form, this becomes

$$\overline{F}_0(\overline{\beta},\mathbf{Q},\mathbf{B}) = \frac{1}{2}(\mathbf{Q}\cdot\mathbf{Q} + 2\gamma\,\mathbf{Q}\cdot\mathbf{B} + \lambda\,\mathbf{B}\cdot\mathbf{B}) \\ -\frac{1}{\overline{\beta}}\ln\frac{1}{|\Omega|}\int_\Omega e^{\overline{\beta}\{\mathbf{q}(\omega)\cdot\mathbf{Q}+\gamma[\mathbf{q}(\omega)\cdot\mathbf{B}+\mathbf{b}(\omega)\cdot\mathbf{Q}]+\lambda\mathbf{b}(\omega)\cdot\mathbf{B}\}}d\omega\,, \tag{4.3}$$

where

$$\overline{F}_0 := \frac{F_0}{zU_0}, \quad \overline{\beta} := \frac{zU_0}{k_B T}.$$

The constant factor $|\Omega| = \int_\Omega d\omega = 8\pi^2$, which does not affect the equilibrium phases, has been introduced for normalisation so that $F_0 = 0$ in the isotropic state $\mathbf{Q} = \mathbf{B} = \mathbf{0}$ – we henceforth drop the overbars.

Stationarity of F_0 can be seen to imply self-consistency (except for the degenerate case $\lambda = \gamma^2$):

$$D_{\mathbf{Q}}F_0 = \mathbf{0}\,,\ D_{\mathbf{B}}F_0 = \mathbf{0} \quad \Rightarrow \quad \mathbf{Q} = \langle\mathbf{q}(\cdot)\rangle_{\rho_0},\ \mathbf{B} = \langle\mathbf{b}(\cdot)\rangle_{\rho_0}.$$

In the case of multiple coexisting equilibria, the phase of the system is given by the equilibrium pair $(\mathbf{Q},\mathbf{B})$ that gives the least value of the free energy F_0. At high temperatures (low values of β), the only stationary point of F_0 is given by the isotropic state $\mathbf{Q} = \mathbf{B} = \mathbf{0}$. As the temperature is lowered (β is increased), non-trivial solutions of (4.2) emerge with

https://doi.org/10.1017/S0956792510000355 Published online by Cambridge University Press

lower free-energy values, yielding ordered phases of different types and degrees of order (depending on the nature of **Q** and **B**). We emphasise that while the expression for the mean-field approximate free energy (4.3) makes sense for any real, symmetric and traceless tensors **Q** and **B**, it has a provable relationship to the true free energy of the ensemble only when **Q** and **B** satisfy the self-consistency conditions (4.2).

4.2 Numerical implementation

When the mean-field free energy in (4.3) develops an ordered phase (that is, it is stationary for **Q** or **B** different from zero), it does so in a degenerate way, as **Q** and **B** (and the whole ensemble) can order in any orientation or direction in space. Thus we can fix an eigenframe $\boldsymbol{e}_x$, $\boldsymbol{e}_y$, $\boldsymbol{e}_z$, which we assume both **Q** and **B** share, and represent these symmetric and traceless tensors as

$$\begin{aligned}\mathbf{Q} &= S\left(\boldsymbol{e}_z \otimes \boldsymbol{e}_z - \frac{1}{3}\mathbf{I}\right) + T(\boldsymbol{e}_x \otimes \boldsymbol{e}_x - \boldsymbol{e}_y \otimes \boldsymbol{e}_y),\\ \mathbf{B} &= S'\left(\boldsymbol{e}_z \otimes \boldsymbol{e}_z - \frac{1}{3}\mathbf{I}\right) + T'(\boldsymbol{e}_x \otimes \boldsymbol{e}_x - \boldsymbol{e}_y \otimes \boldsymbol{e}_y).\end{aligned} \tag{4.4}$$

The real variables in $\boldsymbol{x} = (S, T, S', T')$ are 'scalar order parameters' (related to the eigenvalues of **Q** and **B**). In terms of these variables, the isotropic phase corresponds to $S = T = S' = T' = 0$, while the uniaxial nematic phase is given by either $S \neq 0$ or $S' \neq 0$ (or both) together with $T = T' = 0$, and the biaxial nematic phase is associated with $T \neq 0$ and/or $T' \neq 0$. We note that there are actually three equivalent expressions in (S, T, S', T') for each uniaxial state and six for each biaxial one because of the possibility of interchanging the roles of $\boldsymbol{e}_x$, $\boldsymbol{e}_y$ and $\boldsymbol{e}_z$.

In terms of the parameterisation above, the dimensionless mean-field free energy (4.3) takes the following form:

$$F_0(S, T, S', T', \beta) = \frac{1}{3}S^2 + T^2 + 2\gamma\left(\frac{1}{3}SS' + TT'\right) + \lambda\left(\frac{1}{3}S'^2 + T'^2\right) - \frac{1}{\beta}\ln\frac{Z_0}{8\pi^2}, \tag{4.5a}$$

where

$$Z_0(S, T, S', T', \beta) = \int_0^{2\pi}\int_0^{2\pi}\int_0^{\pi} e^{\beta g(\theta,\phi,\psi)}\sin\theta\, d\theta\, d\phi\, d\psi\,, \tag{4.5b}$$

with

$$\begin{aligned}g(\theta, \phi, \psi) = {} & (S + \gamma S')\left(\cos^2\theta - \frac{1}{3}\right) + \sin^2\theta\,[(T + \gamma T')\cos 2\phi + (\gamma S + \lambda S')\cos 2\psi]\\ & + (\gamma T + \lambda T')[(1 + \cos^2\theta)\cos 2\phi\cos 2\psi - 2\cos\theta\sin 2\phi\sin 2\psi]\,.\end{aligned} \tag{4.5c}$$

The function F_0 in (4.5a) is invariant under the transformations of (S, T, S', T') that leave both **Q** and **B** in (4.4) unchanged upon exchanging the members of the basis $(\boldsymbol{e}_x, \boldsymbol{e}_y, \boldsymbol{e}_z)$. In particular, by exchanging $\boldsymbol{e}_x$ and $\boldsymbol{e}_y$, the pair (T, T') is transformed into $(-T, -T')$. As can also be checked directly, such a parity transformation also leaves F_0 unchanged, thus embodying a symmetry of the type considered in this paper. In particular, the corresponding spaces $\mathbb{X}_\mathrm{s}$ and $\mathbb{X}_\mathrm{a}$ that decompose $\mathbb{R}^4$ are here $\mathbb{X}_\mathrm{s} = \{\boldsymbol{x} \in \mathbb{R}^4 \mid \boldsymbol{x} = (S, 0, S', 0)\}$ and $\mathbb{X}_\mathrm{a} = \{\boldsymbol{x} \in \mathbb{R}^4 \mid \boldsymbol{x} = (0, T, 0, T')\}$. Specifically, this $\mathbb{X}_\mathrm{s}$ represents a

https://doi.org/10.1017/S0956792510000355 Published online by Cambridge University Press

collection of uniaxial phases. Two other equivalent flavours of the same collection are obtained from it by applying to (4.4) the transformations that exchange $\boldsymbol{e}_z$ with either $\boldsymbol{e}_x$ or $\boldsymbol{e}_y$. It is easily shown (for example, by use of (38b) of [3]) that the equivalent images of $\mathbb{X}_{\rm s}$ under these transformations are $\mathbb{X}'_{\rm s} = \{\boldsymbol{x} \in \mathbb{R}^4 \mid \boldsymbol{x} = -\frac{1}{2}(S, -S, S', -S')\}$ and $\mathbb{X}''_{\rm s} = \{\boldsymbol{x} \in \mathbb{R}^4 \mid \boldsymbol{x} = -\frac{1}{2}(S, S, S', S')\}$, whence similar expressions for the corresponding orthogonal complements $\mathbb{X}'_{\rm a}$ and $\mathbb{X}''_{\rm a}$ would follow. Our method, which is here applied to the symmetry-breaking bifurcations into $\mathbb{X}_{\rm a}$, would equally apply to the corresponding bifurcations of the replicas $\mathbb{X}'_{\rm s}$ and $\mathbb{X}''_{\rm s}$ of $\mathbb{X}_{\rm s}$ into $\mathbb{X}'_{\rm a}$ and $\mathbb{X}''_{\rm a}$, respectively. We shall hereafter disregard these equivalent bifurcation replicas, with no loss in generality.

Free energies are calculated using formulas (4.5) (after some simplifications) with a high-order quadrature rule used to approximate the triple integral. The stationarity conditions are a coupled system of four nonlinear equations in the four unknowns (S, T, S', T') resulting from

$$\nabla_{\boldsymbol{x}} F_0 = \boldsymbol{0} \quad \Leftrightarrow \quad \frac{\partial F_0}{\partial S} = \frac{\partial F_0}{\partial T} = \frac{\partial F_0}{\partial S'} = \frac{\partial F_0}{\partial T'} = 0\,.$$

For given material parameters, γ and λ, solution branches are explored with the aid of a numerical bifurcation package, MatCont (see http://sourceforge.net/projects/matcont/), with β as continuation parameter. The isotropic state, $S = T = S' = T' = 0$, is always an equilibrium solution for any value of β. All non-trivial solutions that we have been able to find were obtained by following branches (including secondary bifurcations) bifurcating from the isotropic (trivial) branch.

As branches of equilibria are traced out numerically, free energies are tabulated and local stability is assessed at each computed solution point. The tabulated free energies are used to determine the globally stable phase of the system. The assessment of local stability involves the eigenvalues of the Hessian of F_0 with respect to S, T, S' and T'. In some cases (depending on the values of γ and λ) this is simply a matter of determining if the minimum eigenvalue of the Hessian is non-negative. In other cases, for values of γ and λ associated with 'partly repulsive' pair potentials, the criterion for local stability is more subtle and involves the non-negativity of an eigenvalue of the Hessian other than the minimum one – see [1,5]. As branches of equilibria are traced out, the ξ and τ parameters of Section 3.1 are also calculated to identify potential tricritical points. We now sketch how the calculation of ξ and τ is performed.

We consider a bifurcation breaking the $\mathbb{Z}_2$ symmetry $(T, T') \mapsto (-T, -T')$ at a point $P_0 = (\boldsymbol{x}_0, \beta_0)$ with a rank defect of one, as discussed in Section 3.1.1. Thus the Hessian of F_0 is singular at P_0 and has a one-dimensional kernel $\mathbb{K} \subset \mathbb{X}_{\rm a}$. The formulas for ξ and τ are given by (3.10) and (3.11), which for the purpose of numerical evaluation we write as

$$\xi = \left[\nabla^3_{\boldsymbol{x}} F(\boldsymbol{x}_0, \beta_0) \cdot (\boldsymbol{t}_0 \otimes \boldsymbol{t}_0)\right] \cdot \mathbf{H}_{0\rm s}^{-1} \boldsymbol{b}_0 - \mathbf{B}_0 \boldsymbol{t}_0 \cdot \boldsymbol{t}_0 \tag{4.6}$$

and

$$\begin{aligned} \tau = {} & \nabla^4_{\boldsymbol{x}} F(\boldsymbol{x}_0, \beta_0) \cdot (\boldsymbol{t}_0 \otimes \boldsymbol{t}_0 \otimes \boldsymbol{t}_0 \otimes \boldsymbol{t}_0) \\ & -3 \left[\nabla^3_{\boldsymbol{x}} F(\boldsymbol{x}_0, \beta_0) \cdot (\boldsymbol{t}_0 \otimes \boldsymbol{t}_0)\right] \cdot \mathbf{H}_{0\rm s}^{-1} \left[\nabla^3_{\boldsymbol{x}} F(\boldsymbol{x}_0, \beta_0) \cdot (\boldsymbol{t}_0 \otimes \boldsymbol{t}_0)\right]. \end{aligned} \tag{4.7}$$

The role of F is now being played by the mean-field free energy F_0 of (4.5a). By computing explicitly τ in (4.7) and requiring it to vanish, one recovers the tricriticality criterion worked out in [6] (see (4.4)) within a theory limited to condensed phases described at most by

https://doi.org/10.1017/S0956792510000355 Published online by Cambridge University Press

four scalar order parameters. In our numerical implementation of the search for general symmetric tricritical points with $\dim \mathbb{K} = 1$, we found it convenient to restore $\overline{\mathbf{H}_0^{-1}}$ in both (4.6) and (4.7) instead of $\mathbf{H}_{s0}^{-1}$, which has there the same effect. We found this method more appealing for its genericness, as only $\mathbf{H}_0$ and $\boldsymbol{t}_0$ need to be known numerically for it to apply: such a feature becomes more valuable when the method is applied to retrace the bifurcation branches emanating from the other two equivalent uniaxial states related to the one being considered here by the three-fold symmetry enjoyed by the representation of $\mathbf{Q}$ and $\mathbf{B}$ in (4.4).

The numerical bifurcation package that we have employed requires user-supplied functions to evaluate the equilibrium equations and some higher derivative information. This information is expressed in terms of coordinate vectors and matrices with respect to the standard bases:

$$F = F(\boldsymbol{x}, \boldsymbol{p}), \quad \boldsymbol{x} = (S, T, S', T') \quad \boldsymbol{p} = (\beta, \gamma, \lambda)$$
$$\mathsf{g} := \left[\frac{\partial F}{\partial x_i}\right]_{4\times 1}, \quad \mathsf{H} := \left[\frac{\partial^2 F}{\partial x_i \partial x_j}\right]_{4\times 4}, \quad \mathsf{H}_p := \left[\frac{\partial^2 F}{\partial x_i \partial p_j}\right]_{4\times 3}.$$

The formulas for these were developed analytically from (4.5), with a high-order quadrature rule used to evaluate the various triple integrals that occur in all these expressions. Note that g and H are just the coordinate vector and matrix for the gradient $\boldsymbol{G}$ and the Hessian $\mathbf{H}$, respectively. Note also that the first column of the H_p matrix is just the coordinate vector for $\boldsymbol{b} = \frac{\partial}{\partial \beta} \nabla_{\boldsymbol{x}} F$. These routines are available to be called to evaluate any of these quantities, as needed, for any values of $(S, T, S', T', \beta, \gamma, \lambda)$. We base our computations of ξ and τ upon them.

The evaluation of ξ and τ begins by first calling the user-supplied function to evaluate the Hessian matrix H_0 at P_0, and then using a library routine to calculate its eigenvalues and orthonormal eigenvectors:

$$\mathsf{H}_0 \mathsf{u}_i = \lambda_i \mathsf{u}_i, \ i = 1, 2, 3, 4, \quad \mathsf{u}_j^{\mathsf{T}} \mathsf{u}_i = \delta_{ij}, \quad \lambda_1 = 0, \ \lambda_2, \lambda_3, \lambda_4 \neq 0.$$

From these we build

$$\mathsf{t}_0 = \mathsf{u}_1, \quad \mathsf{Q} = [\mathsf{u}_2, \mathsf{u}_3, \mathsf{u}_4].$$

The column vector t_0 is the coordinate vector of the tangent to the bifurcating branch, and the columns of the 4×3 matrix Q form an orthonormal basis for the column space of H_0. In terms of Q, one can express the matrix representation of the orthogonal projection onto $\mathbb{K}_\perp$ (which coincides with the range of $\mathbf{H}_0$) and the inverse of $\mathbf{H}_0$ restricted to its range:

$$[\mathbf{P}_{\mathbb{K}_\perp}] = \mathsf{Q}\mathsf{Q}^{\mathsf{T}}, \quad \left[\overline{\mathbf{H}_0^{-1}}\right] = \mathsf{Q}\left(\mathsf{Q}^{\mathsf{T}}\mathsf{H}_0\mathsf{Q}\right)^{-1}\mathsf{Q}^{\mathsf{T}}.$$

For the computation of both the ξ and τ formulas, we require the vector $\nabla_{\boldsymbol{x}}^3 F(\boldsymbol{x}_0, \beta_0) \cdot (\boldsymbol{t}_0 \otimes \boldsymbol{t}_0)$. In order to evaluate this, it is helpful to observe that it corresponds to the second directional derivative of the gradient $\boldsymbol{G}$ in the direction $\boldsymbol{t}_0$:

$$\nabla_{\boldsymbol{x}}^3 F(\boldsymbol{x}_0, \beta_0) \cdot (\boldsymbol{t}_0 \otimes \boldsymbol{t}_0) = \frac{d^2}{d\varepsilon^2} \boldsymbol{G}(\boldsymbol{x}_0 + \varepsilon \boldsymbol{t}_0, \beta_0)\Big|_{\varepsilon=0}.$$

https://doi.org/10.1017/S0956792510000355 Published online by Cambridge University Press

Let v denotes the associated coordinate vector, which we can approximate by standard central finite differences:

$$\mathsf{v} = \frac{d^2}{d\varepsilon^2}\mathsf{g}(\boldsymbol{x}_0 + \varepsilon\,\boldsymbol{t}_0, \beta_0)\bigg|_{\varepsilon=0} \approx \frac{1}{\varepsilon^2}[\,\mathsf{g}(\boldsymbol{x}_0 + \varepsilon\,\boldsymbol{t}_0, \beta_0) - 2\mathsf{g}(\boldsymbol{x}_0, \beta_0) + \mathsf{g}(\boldsymbol{x}_0 - \varepsilon\,\boldsymbol{t}_0, \beta_0)]\,.$$

The middle term in brackets above vanishes at all equilibrium points, and we obtain our final approximate formula for this vector:

$$\tilde{\mathsf{v}} := \frac{1}{\delta_2^2}[\,\mathsf{g}(\boldsymbol{x}_0 + \delta_2\boldsymbol{t}_0, \beta_0) + \mathsf{g}(\boldsymbol{x}_0 - \delta_2\boldsymbol{t}_0, \beta_0)].$$

Here the evaluations of g are performed by the user gradient routine, and the step size δ_2 is chosen to give machine-attainable accuracy. The coordinate vector associated with $\overline{\mathbf{H}_0^{-1}}(\nabla_{\boldsymbol{x}}^3 F(\boldsymbol{x}_0, \beta_0)\cdot(\boldsymbol{t}_0\otimes\boldsymbol{t}_0))$, which we call w, can then be approximated via

$$\mathsf{w} = \left[\,\overline{\mathbf{H}_0^{-1}}\left(\nabla_{\boldsymbol{x}}^3 F(\boldsymbol{x}_0, \beta_0)\cdot(\boldsymbol{t}_0\otimes\boldsymbol{t}_0)\right)\,\right] = \mathsf{Q}(\mathsf{Q}^{\mathsf{T}}\mathsf{H}_0\mathsf{Q})^{-1}\mathsf{Q}^{\mathsf{T}}\mathsf{v} \approx \mathsf{Q}(\mathsf{Q}^{\mathsf{T}}\mathsf{H}_0\mathsf{Q})^{-1}\mathsf{Q}^{\mathsf{T}}\tilde{\mathsf{v}} =: \tilde{\mathsf{w}}$$

by solving a three-by-three linear algebraic system.

The value of $\nabla_{\boldsymbol{x}}^4 F(\boldsymbol{x}_0, \beta_0)\cdot(\boldsymbol{t}_0\otimes\boldsymbol{t}_0\otimes\boldsymbol{t}_0\otimes\boldsymbol{t}_0)$ can be approximated in a similar way by observing that

$$\begin{aligned}\nabla_{\boldsymbol{x}}^4 F(\boldsymbol{x}_0, \beta_0)\cdot(\boldsymbol{t}_0\otimes\boldsymbol{t}_0\otimes\boldsymbol{t}_0\otimes\boldsymbol{t}_0)\\ = \frac{\partial^4 F}{\partial x_i\partial x_j\partial x_k\partial x_l}\bigg|_{P_0} t_i^0\,t_j^0\,t_k^0\,t_l^0 = t_i^0\left[\frac{\partial^2 \mathsf{H}_{ij}}{\partial x_k\partial x_l}\bigg|_{P_0} t_k^0\,t_l^0\right] t_j^0\,.\end{aligned}$$

The expression in brackets above can be related to the second directional derivative of H_{ij} in the direction $\boldsymbol{t}_0$:

$$\frac{d^2}{d\varepsilon^2}\mathsf{H}_{ij}(\boldsymbol{x}_0 + \varepsilon\,\boldsymbol{t}_0, \beta_0)\bigg|_{\varepsilon=0} = \frac{\partial^2 \mathsf{H}_{ij}}{\partial x_k\partial x_l}\bigg|_{P_0} t_k^0\,t_l^0\,.$$

Again this can be approximated by standard central differences to obtain

$$\begin{aligned}\nabla_{\boldsymbol{x}}^4 F(\boldsymbol{x}_0, \beta_0)\cdot(\boldsymbol{t}_0\otimes\boldsymbol{t}_0\otimes\boldsymbol{t}_0\otimes\boldsymbol{t}_0)\\ \approx \frac{1}{\delta_2^2}\mathsf{t}_0^{\mathsf{T}}\,[\mathsf{H}(\boldsymbol{x}_0 + \delta_2\boldsymbol{t}_0, \beta_0) - 2\mathsf{H}(\boldsymbol{x}_0, \beta_0) + \mathsf{H}(\boldsymbol{x}_0 - \delta_2\boldsymbol{t}_0, \beta_0)]\,\mathsf{t}_0\,.\end{aligned}$$

The matrix $\mathsf{H}_0 = \mathsf{H}(\boldsymbol{x}_0, \beta_0)$ has already been evaluated. The other two needed Hessian matrices can be evaluated via the user Hessian routine, and we arrive at our final approximation to the τ formula (4.7):

$$\tau \approx \frac{1}{\delta_2^2}\mathsf{t}_0^{\mathsf{T}}\,[\mathsf{H}(\boldsymbol{x}_0 + \delta_2\boldsymbol{t}_0, \beta_0) - 2\mathsf{H}_0 + \mathsf{H}(\boldsymbol{x}_0 - \delta_2\boldsymbol{t}_0, \beta_0)]\,\boldsymbol{t}_0 - 3\tilde{\mathsf{w}}^{\mathsf{T}}\tilde{\mathsf{v}}\,. \tag{4.8}$$

Again the step size δ_2 is chosen to give machine-attainable accuracy.

The values of ξ can be similarly calculated. The coordinate vector $\mathsf{b}_0 = [\boldsymbol{b}_0] = [\frac{\partial}{\partial\beta}\nabla_{\boldsymbol{x}} F(\boldsymbol{x}_0, \beta_0)]$ is obtained from the first column of the matrix H_p returned by the user

https://doi.org/10.1017/S0956792510000355 Published online by Cambridge University Press

routine. The coordinate vector $\mathsf{r} = [\overline{\mathbf{H}_0^{-1}\boldsymbol{b}_0}]$ is computed in the same way that w was calculated from v above:

$$\mathsf{r} = \left[\overline{\mathbf{H}_0^{-1}\boldsymbol{b}_0}\right] = \mathsf{Q}\left(\mathsf{Q}^{\mathsf{T}}\mathsf{H}_0\mathsf{Q}\right)^{-1}\mathsf{Q}^{\mathsf{T}}\mathsf{b}_0\,.$$

The matrix $\mathsf{B}_0 = [\frac{\partial}{\partial\beta}\nabla_{\boldsymbol{x}}^2 F(\boldsymbol{x}_0, \beta_0)]$ can be approximated by centred differences with respect to β:

$$\mathsf{B}_0 \approx \frac{1}{2\delta_1}\left[\mathsf{H}(\boldsymbol{x}_0, \beta_0 + \delta_1) - \mathsf{H}(\boldsymbol{x}_0, \beta_0 - \delta_1)\right] =: \widetilde{\mathsf{B}}_0\,,$$

where again the user Hessian routine is called for the evaluations of H, and δ_1 is chosen to deliver machine-attainable accuracy. The final approximation for the ξ formula (4.6) is given by

$$\xi \approx \mathsf{r}^{\mathsf{T}}\tilde{\mathsf{v}} - \mathsf{t}_0^{\mathsf{T}}\widetilde{\mathsf{B}}_0\mathsf{t}_0\,. \tag{4.9}$$

The limiting factor in the accuracy of these formulas is the accuracy to which the user functions evaluate $\partial F/\partial x_i$, $\partial^2 F/\partial x_i \partial x_j$ and $\partial^2 F/\partial x_i \partial\beta$. With the finite-difference step sizes δ_1 and δ_2 properly calibrated, the computed τ and ξ should have no worse than half the precision of the outputs of the user routines. In our implementation, the quadrature used for the triple integrals in the user routines delivers close to full floating-point double-precision accuracy (around 14–15 significant digits), and so the computed values of τ and ξ should have around seven significant digits.

Further advantage of the one-dimensional nature of the kernel of $\mathbf{H}_0$ could be taken by computing $\tilde{\mathsf{w}}$ and r using the (non-singular) bordered systems,

$$\begin{bmatrix}\mathsf{H}_0 & \mathsf{t}_0\\ \mathsf{t}_0^{\mathsf{T}} & 0\end{bmatrix}\begin{bmatrix}\tilde{\mathsf{w}}\\ u\end{bmatrix} = \begin{bmatrix}\tilde{\mathsf{v}}\\ 0\end{bmatrix}, \quad \begin{bmatrix}\mathsf{H}_0 & \mathsf{t}_0\\ \mathsf{t}_0^{\mathsf{T}} & 0\end{bmatrix}\begin{bmatrix}\mathsf{r}\\ u\end{bmatrix} = \begin{bmatrix}\mathsf{b}_0\\ 0\end{bmatrix}, \tag{4.10}$$

which uniquely determine $\tilde{\mathsf{w}}$ and r via

$$\mathsf{H}_0\tilde{\mathsf{w}} = \tilde{\mathsf{v}},\ \mathsf{t}_0^{\mathsf{T}}\tilde{\mathsf{w}} = 0, \quad \mathsf{H}_0\mathsf{r} = \mathsf{b}_0,\ \mathsf{t}_0^{\mathsf{T}}\mathsf{r} = 0,$$

with $u = 0$ in each case. This is more consistent with common practice in numerical bifurcation theory – see [9 (ch. 3), 16 (pp. 176–177)].

In the numerical phase and bifurcation analysis of the biaxial mean-field model expressed in (4.5), tricritical points are encountered in multiple places. One such encounter is associated with a phase sequence, in which a high-temperature isotropic phase, upon cooling, suffers a first-order transition to a uniaxial phase associated with a branch that bifurcates from the isotropic branch at a slightly lower temperature (slightly larger value of β). This uniaxial branch then suffers a secondary bifurcation to a biaxial branch as the temperature is further lowered. For small values of the biaxiality parameter λ, this secondary bifurcation is supercritical and is associated with a second-order uniaxial–biaxial phase transition. For larger values of λ, this bifurcation becomes subcritical, and the transition becomes first-order transition. The value of λ (and associated critical value of β) at which the change from supercritical (second-order) to subcritical (first-order) occurs corresponds to a tricritical point of the precise nature analysed in Section 3.1.

The primary order parameters that play a role in this particular phase sequence are S and T'. Figures 3–5 illustrate the supercritical, tricritical and subcritical sequences as

https://doi.org/10.1017/S0956792510000355 Published online by Cambridge University Press

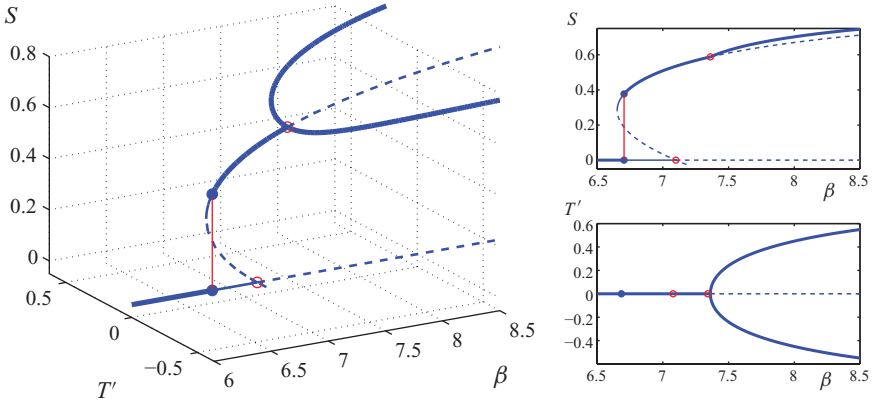

FIGURE 3. (Colour online) Bifurcation diagram for the biaxial mean-field free energy F_0 in (4.5a): supercritical case ($\gamma = 0.1$, $\lambda = 0.175$). Dominant-order parameters: S, T'. Isotropic branch: $S = T' = 0$. Uniaxial branch: $S \neq 0$, $T' = 0$. Biaxial branch: $T' \neq 0$. Critical parameter values are given in Table 4.2. Dashed lines: unstable equilibria; solid lines: locally stable; heavy solid lines: globally stable.

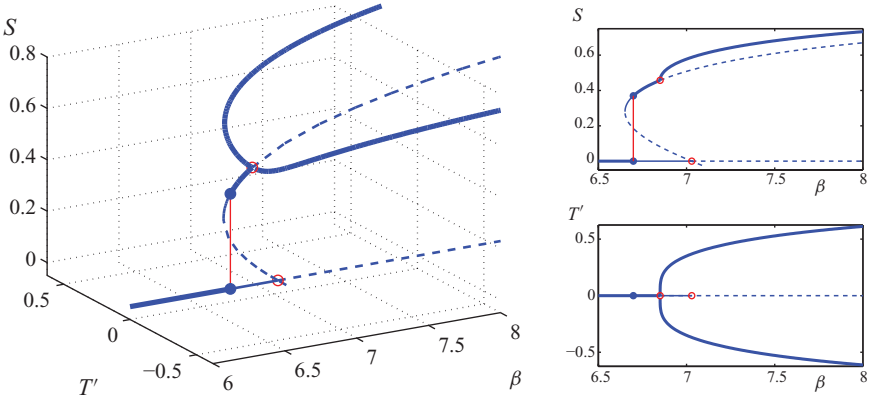

FIGURE 4. (Colour online) Bifurcation diagram for biaxial mean-field free energy F_0 in (4.5a): tricritical case ($\gamma = 0.1$, $\lambda = 0.206$). Dominant-order parameters: S, T'. Isotropic branch: $S = T' = 0$. Uniaxial branch: $S \neq 0$, $T' = 0$. Biaxial branch: $T' \neq 0$. Critical parameter values are given in Table 4.2. Dashed lines: unstable equilibria; solid lines: locally stable; heavy solid lines: globally stable.

λ changes from 0.175 to 0.206 to 0.215 (with fixed $\gamma = 0.1$). The values of ξ and τ at the bifurcation point, computed using formulas (4.9) and (4.8), are summarised in Table 4.2 and indicate the proper sign patterns associated with the criterion developed in Section 3.2.1. Further increase in the λ parameter results in the biaxial branch superseding the uniaxial one, accompanied by the direct first-order isotropic-biaxial transition [1]. It should finally be recalled that, as already mentioned above, there are two other uniaxial branches equivalent to this one (related to interchanged roles of $\boldsymbol{e}_x$, $\boldsymbol{e}_y$ and $\boldsymbol{e}_z$) and associated symmetry-breaking secondary bifurcations corresponding to different values of (S, T, S', T') that exactly present the same picture.

https://doi.org/10.1017/S0956792510000355 Published online by Cambridge University Press

Table 1. *Parameter values associated with phase sequences illustrated in Figures 3–5; γ and λ are dimensionless model parameters associated with the biaxial mean-field model* (4.5)*; β_0 corresponds to the value of continuation parameter β (reduced reciprocal temperature) at the secondary bifurcation from the uniaxial ($T' = 0$) to the biaxial ($T' \neq 0$) branch; ξ and τ are the values of the parameters associated with the tricriticality criterion defined in* (3.10) *and* (3.11) *and evaluated by* (4.9) *and* (4.8)

Figure	γ	λ	β_0	ξ	τ
3	0.1	0.175	7.362	0.889	1.114
4	0.1	0.206	6.850	0.183	0.000
5	0.1	0.215	6.767	0.241	−1.282

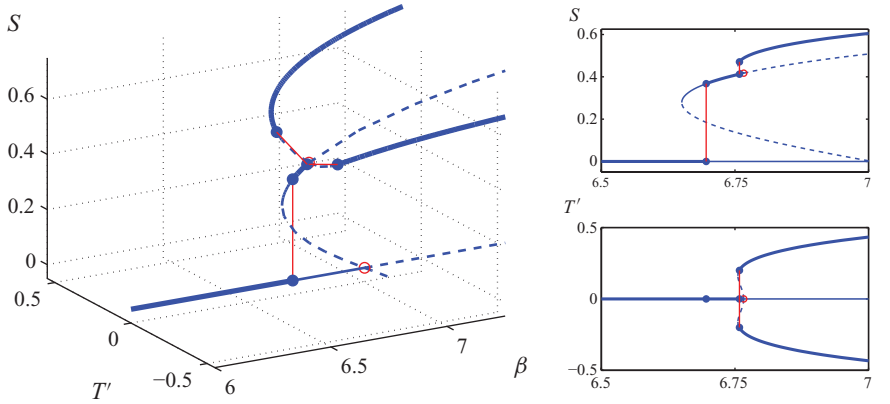

FIGURE 5. (Colour online) Bifurcation diagram for biaxial mean-field free energy F_0 in (4.5a): subcritical case ($\gamma = 0.1$, $\lambda = 0.215$). Dominant-order parameters S, T'. Isotropic branch: $S = T' = 0$. Uniaxial branch: $S \neq 0$, $T' = 0$. Biaxial branch: $T' \neq 0$. Critical parameter values are given in Table 4.2. Dashed lines: unstable equilibria; solid lines: locally stable; heavy solid lines: globally stable.

5 Conclusions

We considered symmetric tricritical points, where an ordering phase transition changes from first to second order, or *vice versa*. We pointed out how the origin of this name – tricritical – can be retraced in the language of phase coexistence and how it came to acquire the broader meaning adopted here, especially in the liquid crystal literature, where tricritical points have been both predicted theoretically [24] and observed experimentally [23]. We reviewed classical methods of bifurcation theory and applied them to the issue at hand, intending to arrive at a simple analytical criterion that indicates where tricritical points may take place along a phase represented by a family of (possibly temperature-depending) stationary points for a free energy F expressed in terms of any finite number of scalar order parameters, be it derived from a mean-field approximation or suggested by a Landau theory.

We fully succeeded in our objective only when the equilibrium solutions representing a competing phase bifurcate at a point where the Hessian of F has a null space $\mathbb{K}$ of

https://doi.org/10.1017/S0956792510000355 Published online by Cambridge University Press

dimension one. Our analysis of the bifurcation equations was intentionally more general and also allowed for $\dim \mathbb{K} > 1$, to explore possible avenues to extend our criterion, which, however, remains fully predictive only for $\dim \mathbb{K} = 1$.

A feature of the types of problems we consider, which distinguishes them from more general problems of equivariant bifurcation theory, is that they are gradient systems, for which the equilibrium equations derive from energy (or free energy, in our case). This provides additional structure, as, for example, the Jacobian associated with the equilibrium equations is actually the Hessian, and therefore symmetric with orthogonal kernel, range etc. The setting is similar to that found in computational mechanics, for example [13] or [27]. In the latter paper, an energy-derived system is analysed via the Lyapunov–Schmidt reduction and questions related to the stability of bifurcating branches are also considered. What is referred to in that paper as 'the symmetric case' is analogous to the type of symmetry breaking that we have considered here. The approach of [27] is somewhat more algebraic and coordinate-based, however, and aspects different from those considered here are explored there.

As is clear from its formulation (3.23), the tricriticality criterion proposed here is of a local nature, as it only indicates whether a transition, in case it really takes place at the bifurcation point under scrutiny, is of first or second order. In order to know whether a putative first- or second-order transition actually takes place, one should also assess information of a global nature. As already remarked in Section 3.1, a necessary condition is that the branch representing the competing phase connects at sufficiently low temperatures with the ground state of F. Even this, however, is not sufficient, and other bifurcations away from the one being followed may realise the least stationary value of F at the given temperature. Nevertheless, as shown by the explicit implementation of the criterion in Section 4.2, monitoring τ and ξ along all branches explored numerically provides a complete inventory of the bifurcation points that may become tricritical points.

If the limitation of our criterion connected to its local nature can be circumvented by systematic exploration of the equilibrium branches connected with the free-energy ground state, then the limitation arising from the assumption that $\dim \mathbb{K} = 1$ is intrinsic. In the mean-field model for biaxial nematics, illustrated in Section 4.1, all secondary bifurcations into the biaxial phase enjoy a reflectional symmetry and happened to satisfy the assumption $\dim \mathbb{K} = 1$, so that (3.23) allowed us to identify in [1] all tricritical points of the uniaxial–biaxial transition in the admissible parameter space (γ, λ). The same model, however, reveals a different scenario when the isotropic-uniaxial transition is examined. The relevant bifurcations are no longer symmetric and moreover $\dim \mathbb{K} = 2$ in the generic case. In order to ascertain whether the isotropic-uniaxial transition is of first or second order in the admissible parameter space (γ, λ), we need a bifurcation analysis that follows the same path outlined in Section 2 above, but conforms to different assumptions. Such an analysis, which will be presented elsewhere, shows that only a first-order transition into the uniaxial phase is possible from the isotropic phase for the free energy in (4.5a) for a generic choice of the model parameters (γ, λ). This is a case where a local criterion, like the one presented here, becomes most predictive, as it dictates analytically the order of phase transition, avoiding any speculations based on the absence or presence of discontinuities in the temperature dependence of the order parameters, which are very hard to validate numerically.

Acknowledgements

The work of ECG was supported in part by the National Science Foundation (USA), grant DMS-0608670; the work of FB was supported by the Italian *Gruppo Nazionale per la Fisica Matematica* (INdAM), grants *Progetti Giovani* 2008–2009.

References

[1] Bisi, F., Virga, E. G., Gartland, E. C., Jr., De Matteis, G., Sonnet, A. M. & Durand, G. E. (2006) Universal mean-field phase diagram for biaxial nematics obtained from a minimax principle. *Phys. Rev. E* **73**, 051709.
[2] Chow, S.-N. & Hale, J. K. (1982) *Methods of Bifurcation Theory*, Springer-Verlag, New York.
[3] De Matteis, G., Bisi, F. & Virga, E. G. (2007) Constrained stability for biaxial nematic phases. *Contin. Mech. Thermodyn.* **19**, 1–23.
[4] De Matteis, G. & Virga, E. G. (2005) Tricritical points in biaxial liquid crystal phases. *Phys. Rev. E* **71**, 061703.
[5] Gartland, E. C., Jr., & Virga, E. G. (2010) Minimum principle for indefinite mean-field free energies. *Arch. Ration. Mech. Anal.* **196**, 143–189.
[6] Gibelli, L. & Turzi, S. (2009) A catastrophe-theoretic approach to tricritical points with applications to liquid crystals. *SIAM J. Appl. Math.* **70**, 63–76.
[7] Golubitsky, M. & Schaeffer, D. G. (1985) *Singularities and Groups in Bifurcation Theory, Vol. I*, Springer-Verlag, Berlin, Germany.
[8] Golubitsky, M., Stewart, I. & Schaeffer, D. G. (1988) *Singularities and Groups in Bifurcation Theory, Vol. II*, Springer-Verlag, Berlin, Germany.
[9] Govaerts, W. J. F. (2000) *Numerical Methods for Bifurcations of Dynamical Equilibria*, SIAM, Philadelphia, PA.
[10] Griffiths, R. B. (1973) Proposal for notation at tricritical points. *Phys. Rev. B* **7**, 545–551.
[11] Griffiths, R. B. (1974) Thermodynamic model for tricritical points in ternary and quaternary fluid mixtures. *J. Chem. Phys.* **60**, 195–206.
[12] Griffiths, R. B. & Widom, B. (1973) Multicomponent-fluid tricritical points. *Phys. Rev. A* **8**, 2173–2175.
[13] Healey, T. J. (1988) A group-theoretic approach to computational bifurcation problems with symmetry. *Comput. Methods Appl. Mech. Eng.* **67**, 257–295.
[14] Keller, H. B. & Langford, W. F. (1972) Iterations, perturbations and multiplicities for nonlinear bifurcation problems. *Arch. Ration. Mech. Anal.* **48**, 83–108.
[15] Kuznetsov, Y. A. (2004) *Elements of Applied Bifurcation Theory,* 3rd ed., Springer, New York.
[16] Laurie, I. D. & Sarbach, S. (1984) Theory of tricritical points. In: C. Domb & J. L. Lebowitz (editors), *Phase Transitions and Critical Phenomena,* Vol. 9, Academic Press, New York.
[17] Longa, L. (1986) On the tricritical point of the nematic-smectic *A* phase transition in liquid crystals. *J. Chem. Phys.* **85**, 2974–2985.
[18] Longa, L. (1989) Order-parameter theories of phase diagrams for antiferroelectric smectic-*A* phases: Role of orientational degrees of freedom. *Liq. Cryst.* **5**, 443–461.
[19] Longa, L., Grzybowski, P., Romano, S. & Virga, E. G. (2005) Minimal coupling model of the biaxial nematic phase. *Phys. Rev. E* **71**, 051714.
[20] Luckhurst, G. R. (2004) Liquid crystals – a missing phase found at last? *Nature (London)* **430**, 413–414.
[21] Maier, W. & Saupe, A. (2004) A simple molecular theory of the nematic liquid-crystalline state. In: T. J. Sluckin, D. A. Dunmur & H. Stegemeyer (editors), *Crystals That Flow: Classic Papers from the History of Liquid Crystals*, Taylor & Francis, London, pp. 380–387 (1958 trans.).
[22] Maier, W. & Saupe, A. (1958) Eine einfache molekulare. Theorie des nematischen kristallinflüssigen Zustandes. Z. Nat. Forsch. **13a**, 564–566.

[23] Merkel, K., Kocot, A., Vij, J. K., Korlacki, R., Mehl, G. H. & Meyer, T. (2004) Thermotropic biaxial nematic phase in liquid crystalline organo-siloxane tetrapodes. *Phys. Rev. Lett*. **93**, 237801.
[24] McMillan, W. L. (1971) Simple molecular model for the smectic *A* phase of liquid crystals. *Phys. Rev*. A **4**, 1238–1246.
[25] Sonnet, A. M., Virga, E. G. & Durand, G. E. (2003) Dielectric shape dispersion and biaxial transitions in nematic liquid crystals. *Phys. Rev. E* **67**, 061701.
[26] Straley, J. P. (1974) Ordered phases of a liquid of biaxial particles. *Phys. Rev. A* **10**, 1881–1887.
[27] Triantafyllidis, N. & Peek, R. (1992) On stability and the worst imperfection shape in solids with nearly simultaneous eigenmodes. *Int. J. Solids Struct*. **29**, 2281–2299.
[28] Vainberg, M. M. & Trenogin, V. A. (1962) The methods of Lyapunov and Schmidt in the theory of non-linear equations and their further development. *Russ. Math. Survs*. **17**, 1–60.
[29] Vainberg, M. M. & Trenogin, V. A. (1974) *Theory of Branching of Solutions of Non-Linear Equations*, Noordhoff, Leyden, the Netherlands.
[30] Widom, B. (1996) Theory of phase equilibrium. *J. Phys. Chem*. **100**, 13190–13199.
[31] Yeomans, J. M. (1992) *Statistical Mechanics of Phase Transitions*, Oxford University Press, Oxford, UK.
[32] Yu, L. J. & Saupe, A. (1980) Observation of a biaxial nematic phase in Potassium Laurate-1-Decanol-water mixtures. *Phys. Rev. Lett*. **45**, 1000–1003.